

# Using multiple archives to understand past and present climate–human–environment interactions: the lake Erhai catchment, Yunnan Province, China

J. A. Dearing · R. T. Jones · J. Shen · X. Yang · J. F. Boyle ·  
G. C. Foster · D. S. Crook · M. J. D. Elvin

Received: 8 October 2007 / Accepted: 26 November 2007  
© Springer Science+Business Media B.V. 2007

**Abstract** A 6.48 m sediment core sequence from Erhai lake, Yunnan Province, provides a multi-proxy record of Holocene environmental evolution and human activity in southwest China. These sedimen-

tary records provide proxy time series for catchment vegetation, flooding, soil erosion, sediment sources and metal workings. They are complemented by independent regional climate time-series from speleothems, archaeological records of human habitation, and a detailed documented environmental history. The article attempts to integrate these data sources to provide a Holocene scale record of environmental change and human–environment interactions. These interactions are analysed in order to identify the roles of climate and social drivers on environmental change, and the lessons that may be learned about the future sustainability of the landscape. The main conclusions are: lake sediment evidence for human impacts from at least 7,500 cal year BP is supported by a terrestrial record of cultural horizons that may extend back to ~9,000 cal year BP. A major shift in the pollen assemblage, defined by detrended correspondence analysis, at ~4,800 cal year BP marks the transition from a ‘nature-dominated’ to a ‘human-dominated’ landscape. From 4,300 cal year BP, a change in river discharge responses may signal the beginning of hydraulic modification through drainage and irrigation. Major increases in disturbed land taxa and loss of forest taxa from 2,200 cal year BP onward, also associated with the start of significant topsoil erosion, register the expansion of agriculture by Han peoples. It is also the start of silver smelting linked to trade along the SW Silk Road with Dali becoming a regional centre. Peak levels of disturbed land taxa, topsoil and gully erosion are associated

---

This article is based on a keynote address delivered by John Dearing at the 10th International Paleolimnology Symposium, June 2006, Duluth, Minnesota, USA.

---

J. A. Dearing (✉) · J. F. Boyle · G. C. Foster  
Department of Geography, University of Liverpool,  
Liverpool L69 7ZT, UK  
e-mail: j.dearing@soton.ac.uk

*Present Address:*

J. A. Dearing  
School of Geography, University of Southampton,  
Southampton SO17 1BJ, UK

R. T. Jones  
Department of Geography, University of Exeter,  
Cornwell Campus, Penryn TR10 9EZ, UK

J. Shen · X. Yang  
Nanjing Institute of Geography and Limnology, Chinese  
Academy of Sciences, Nanjing 210008, China

D. S. Crook  
Department of Geography, University of Hertfordshire,  
Hatfield AL10 9AB, UK

M. J. D. Elvin  
Division of Pacific and Asian History, Research School of  
Pacific and Asian Studies, Australian National University,  
Canberra ACT 0200, Australia

with the rise and fall of the Nanzhao (CE 738–902) and Dali (CE 937–1253) Kingdoms, and the documented environmental crisis that occurred in the late Ming and Qing dynasties (CE 1644–1911). The crisis coincides with a stronger summer monsoon, but exploitation of marginal agricultural land is the main driver. These historical perspectives provide insight into the resilience and sustainability of the modern agricultural system. The largest threat comes from high magnitude-low frequency flooding of lower dry farmed terraces and irrigated valley plains. A sustainable future depends on reducing the use of high altitude and steep slopes for grazing and cultivation, maintaining engineered flood defences and terraces, and anticipating the behaviour of the summer monsoon.

**Keywords** Erhai lake · Yunnan · China · Climate–human–environment interactions · Lake sediment · Palaeohydrology · Vegetation and land use · Erosion · Metal workings · Resilience · Sustainability

## Introduction and aims

There is a long tradition of using environmental archives to reconstruct ecological histories. But it has been only in recent years that the case has been made for long-term perspectives to contribute directly to a better understanding of the functioning of *modern* ecosystems and landscapes (e.g. Oldfield and Dearing 2003; Dearing et al. 2006a). For example, long paleoecological and environmental records may provide insight into the trajectories of ‘vulnerability’ (Messerli et al. 2000) and ‘convergence’ (cf. Homer-Dixon 2006) that lead to the present; they have described the nature of long-term system dynamics and nonlinear change (e.g. Dearing and Zolitschka 1999); they have defined reference conditions for conservation or rehabilitation targets (e.g. Bradshaw et al. 2006); they have illuminated how human activity and climate can interact to effectively condition modern process-responses (Foster et al. 2003); and they have enhanced understanding through data-model comparisons (e.g. Anderson et al. 2006).

In part, the case for learning from the past has been driven by the development of theory about the

resilience and sustainability of ecosystems and landscapes. Ed Deevey’s (1984) schematic model of lake ontogeny, described through autogenic and exogenic controls on trophic equilibria, was perhaps the first to combine the theoretical ideas of systems dynamics with empirically reconstructed ecological trajectories and human impacts. It laid foundations for making generalisations about system states and behaviours, like stress, strain and stability: descriptors for the past with relevance to modern ecosystem functioning. Since then, both empirical and theoretical studies of environmental system dynamics (e.g. Gunderson and Holling 2002; Scheffer and Carpenter 2003) confirm the need for long temporal perspectives, especially where the present is conditioned by the past. However, there is no accepted methodological protocol for studying past climate–human–environment relationships in ways that maximise our insight into issues of modern ecological change and future landscape sustainability (Dearing 2006). Therefore, the broad aim of the present work is to address this deficiency by exploring the rich paleoecological and historical database of a lake-catchment ecosystem in SW China, a densely populated landscape vulnerable to flooding, erosion and tectonic activity.

We review previously published material derived from multiple archives. With new field observations and analytical data, we address the nature and form of millennial–centennial human–environment interactions through the Holocene in the context of long-term socio-ecological sustainability. The specific research questions are:

- How sensitive are the studied environmental system processes to climate and human drivers of change?
- Can we observe long-term trajectories of socio-environmental interactions, or periods of social collapse and recovery?
- What are the implications for modern system functioning and future sustainability?

The article is organised around seven sections that focus on: the study site and methods; controls on lake levels; controls on landscape processes over millennial timescales; controls over sub-millennial timescales for three different past periods; and a discussion of the findings from the perspective of socio-ecological functioning.

## Study area, methods and techniques

### Study area

Erhai (25°36′–25°58′ N, 100°05′–100°18′ E) is China's seventh largest lake located in Yunnan Province in SW China (Fig. 1). It lies at 1,974 m above sea level with a combined lake and catchment area of ~2,500 km<sup>2</sup> (Fig. 2; Table 1). The lake sits within an inter-mountain basin, geologically dominated (Fig. 3) by Palaeozoic metamorphics (gneiss/granite and marble) on the west side, and Mesozoic basic volcanic and sedimentary rocks on the east side (Bureau of Geology and Mineral Resources of Yunnan Province 1990; Socquet and Pubellier 2005).

The modern catchment vegetation and land use (Table 1) can be sub-divided into four main groups, the distribution of which reflects the strong altitudinal gradient of the catchment. On the fluvial plain and lakeshore areas the vegetation is exclusively agricultural, with extensive irrigated areas supporting a double-cropping system of rice, wheat, legumes and other vegetables. Up to 2,500 m, the vegetation is primarily semi-humid evergreen broad-leaved forest, a zonal sub-type of subtropical evergreen broad-leaved forest (SEBF: Lin and Walker 1986). The forest is mainly composed of evergreen oaks and chestnuts (*Castanopsis*, *Cyclobalanopsis* and *Lithocarpus*), accompanied by other trees such as

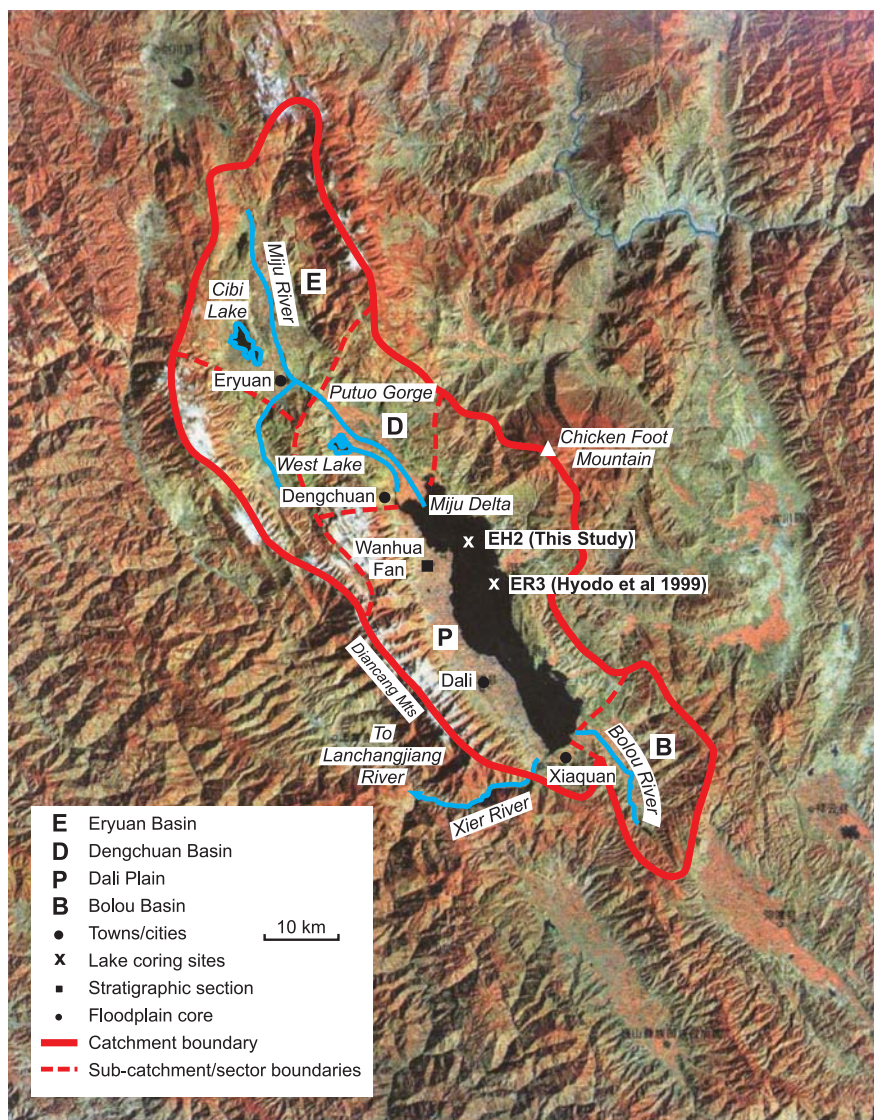
*Pinus yunnanensis* and sclerophyllous *Quercus* as *Q. pannosa*. Due to human disturbance, there is much secondary forest composed primarily of *Pinus yunnanensis* and *Quercus* (Wu et al. 1987). Between 2,500–2,800 m, the cooler temperatures and increased precipitation result in a montane humid evergreen broad-leaved forest, where *Lithocarpus* is the dominant forest taxon with *Castanopsis*, *Cyclobalanopsis*, *Schima*, and *Skimmia* also present. Above 2,800 m this forest type gives way to a mixed conifer woodland, which extends up to ~3,200 m into very high moisture levels. In the Diancangshan mountains, *Tsuga* is frequently mixed with small amounts of other conifers, *Picea*, *Abies* and *Pinus*, and some broad-leaved species, *Quercus*, *Acer* and *Betula*. The understory is typically composed of *Rhododendron* spp., *Sinarundinaria*, *Viburnum*, *Rosa* spp., and some herbs such as *Viola*, *Arisaema* and *Ainsliaea*. Above 3,200 m, *Abies* forest dominates, with *Picea*, *Rhododendron* spp., *Sorbus*, and *Sabina*, although its distribution is patchy.

The catchment may also be sub-divided (Fig. 2) into spatially discrete socio-ecological systems (Elvin et al. 2002). The western side of the lake is dominated by the steep sloped Diancangshan mountains where seasonal snowmelt and springs supply an annual discharge of  $2.76 \times 10^8 \text{ m}^3$  to the Eighteen Streams of the Dali plain, a lower slope system with an extensive off-take diversion irrigation system. To



**Fig. 1** Location of lake Erhai, Dali, the SW Silk Road, Yunnan Province and other sites in southern China referred to in the text (Lake Shayema and Mt Luojie, Sichuan Province; Dongge Cave, Guizhou Province; marine core 17,940, South China Sea)

**Fig. 2** Satellite false colour image of lake Erhai and its catchment showing the catchment boundary, topographic basins, rivers, mountain ranges, lake sediment coring positions and placenames mentioned in the text



the north, the catchment is dominated by the Dengchuan and Eryuan basins with an annual discharge of  $5.18 \times 10^8 \text{ m}^3$  to the lake via the Miju river and a rapidly aggrading delta. The heavily embanked and elevated Miju river provides irrigation water for intensive agriculture on the floodplain. The eastern catchment is dominated by the foothills of Chicken Foot Mountain and is generally dry, treeless and hilly with a sparse population. In contrast, the southern catchment is a prosperous agricultural area based on terraced spring-fed irrigated farming on the floodplain of the Bolou river that has a mean annual discharge of  $1.14 \times 10^8 \text{ m}^3$ . Erhai drains south-westwards via the Xier River into the Lancangjiang

river (Mekong). The lake water quality was classified in the 1980s by Hu et al. (1989) as fresh (conductivity =  $435 \mu\text{S cm}^{-1}$ ) with a pH value of 8.4–8.5, and in 1994 (Whitmore et al. 1997) as oligotrophic ( $5\text{--}10 \mu\text{g l}^{-1}$  total P; conductivity  $216 \mu\text{S cm}^{-1}$ ). Since 1996, the lake has become increasingly mesotrophic due to eutrophication brought about by increased fish production (Whitmore et al. 1997).

A timeline of known human activities derived from archaeological and documentary sources (Table 2) shows that archaeological evidence for early human habitation in the catchment is sparse. A few Neolithic finds were previously found in one excavated alluvial fan on the west side of the lake

**Table 1** Lake and catchment characteristics (Land use data after Wang et al. 2004)

Lake		
Altitude	1,974 m	
Area	150 km <sup>2</sup>	
Mean depth	10.2 m	
Maximum depth	20.7 m	
Volume of	$\sim 2.6 \times 10^9$ m <sup>3</sup>	
Catchment		
Area	2,322 km <sup>2</sup>	
Maximum altitude	4,122 m	
Modern population (1996)	$\sim 800,000$	
Modern land use areas		
Forest	1,048.0 km <sup>2</sup>	(45.1%)
Barren	611.6 km <sup>2</sup>	(26.3%)
Paddy	438.6 km <sup>2</sup>	(18.9%)
Dry land	172.9 km <sup>2</sup>	(7.4%)
Vegetables	28.0 km <sup>2</sup>	(1.2%)
Water	17.0 km <sup>2</sup>	(0.7%)
Urban	4.0 km <sup>2</sup>	(0.2%)
Industry	1.4 km <sup>2</sup>	(0.1%)

(Lin et al. 1986). The local evidence for the regional Bronze Age period ( $\sim 3,000$ – $2,500$  cal year BP) comes from Jianchuan to the north of Erhai (Fig. 1), where bronze axes, sickles, fishhooks, bracelets and ornaments are dated to  $\sim 3,300$  cal year BP (Institute of Archaeology, Yunnan Province 1990). The inward migration and establishment of the Han people (Han Dynasty  $\sim 2,300$ – $1,700$  cal year BP) is represented in the catchment by a single ceramic model found in a grave at the southern end of the lake (Elvin et al. 2002).

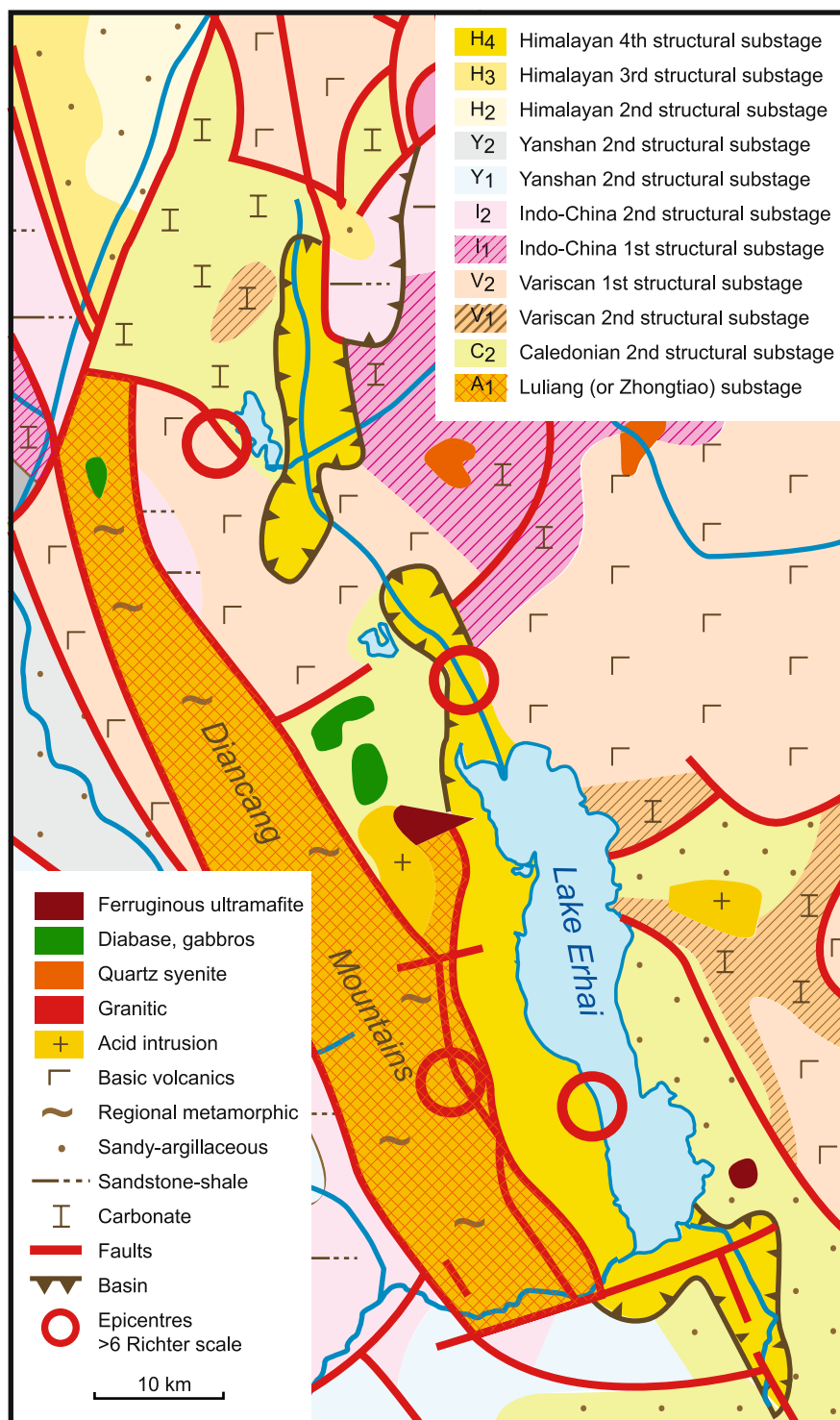
Subsequent periods of human activity in the catchment are better defined in written sources (Elvin et al. 2002). The catchment was the seat of power for the Nanzhao (CE 738–902;  $\sim 1,400$ – $1,000$  cal year BP) and Dali Kingdoms (CE 937–1253;  $\sim 900$ – $600$  cal year BP), both registering peaks in human population, farming and industrial activity, and these in turn were followed by the Ming (CE 1368–1644) and Qing (CE 1644–1911) Dynasties. Within the catchment, population pressure and environmental exploitation rose during the Ming, reaching a well-documented environmental crisis in late Ming/early Qing times ( $\sim 500$ – $200$  cal year BP) characterised by deforestation, catastrophic flooding and erosion (Elvin et al. 2002).

To this evidence of human activity, we can add the results of our recent studies of a 13 m section on the Wanhua alluvial fan on the west shore of the lake (Fig. 2). They reveal  $\sim 12$  dark, relatively fine-grained layers often enriched with organic matter and phosphorus (Fig. 4) which we interpret as transient cultural horizons interbedded with successive flood deposits. Three different types of ceramics from above the eighth lowest cultural horizon are dated by type-comparisons to regional Neolithic cultures with an oldest date of  $\sim 5,000$  <sup>14</sup>C year BP ( $\sim 5,700$  cal year BP: Eldon Worrall, Liverpool Museum pers. comm.) and by radiocarbon on adjacent charcoal to 4,820–4,440 cal year BP (Beta-209867). One of the ceramic types from the cultural horizon above this date is decorated with cord impressions, a style associated with all early rice growing regions of Asia (Kharakwal et al. 2004). A basal date of 9,900–9,570 cal year BP (Beta-190725) on charcoal just below the lowest horizon (sample 61/0) suggests that, at least locally, some form of sedentary agriculture extends well beyond 5,000 cal year BP, possibly as far back as 9,000 cal year BP.

A mean annual temperature of 15.1°C, with small seasonal variation, characterizes the lakeshore climate. Annual precipitation varies greatly according to altitude and location, from 800–900 mm on the relatively dry eastern lake shore to  $>1,800$  mm on the Diancangshan mountains, with 85–90% falling between May and October under the influence of a strong SW summer monsoon that emanates from the Bay of Bengal (Lin and Walker 1986; Wu et al. 1987). During the winter monsoon, winds shift to the north-northwest, bringing mostly dry air to the province. Consequently, winter precipitation between November and March is restricted to disturbance of the polar front and eastward-moving frontal systems.

Previous studies of lake sediments from basins on the Yunnan Plateau, including Erhai, have provided long and continuous palaeoclimate records (Brenner et al. 1991; Fang 1991; Hodell et al. 1999; Long et al. 1991; Whitmore et al. 1994; Yu et al. 1990). Sediment records from northwest Yunnan, supported by modelling studies (Yu et al. 2001; Liu et al. 2002; Chen et al. 2002), show that the Middle Holocene was relatively warm and dry in contrast to the relatively cold and wet conditions at the Last Glacial Maximum. Palynological studies at West lake (Fig. 2) in the Dengchuan basin indicate that the

**Fig. 3** Geology of the Erhai catchment based on the Chinese geological timescale (top right key) and showing dominant rock types, mineralogies, fault lines and epicentres of recently recorded large earthquakes (bottom left key) (Bureau of Geology and Mineral Resources of Yunnan Province 1990)



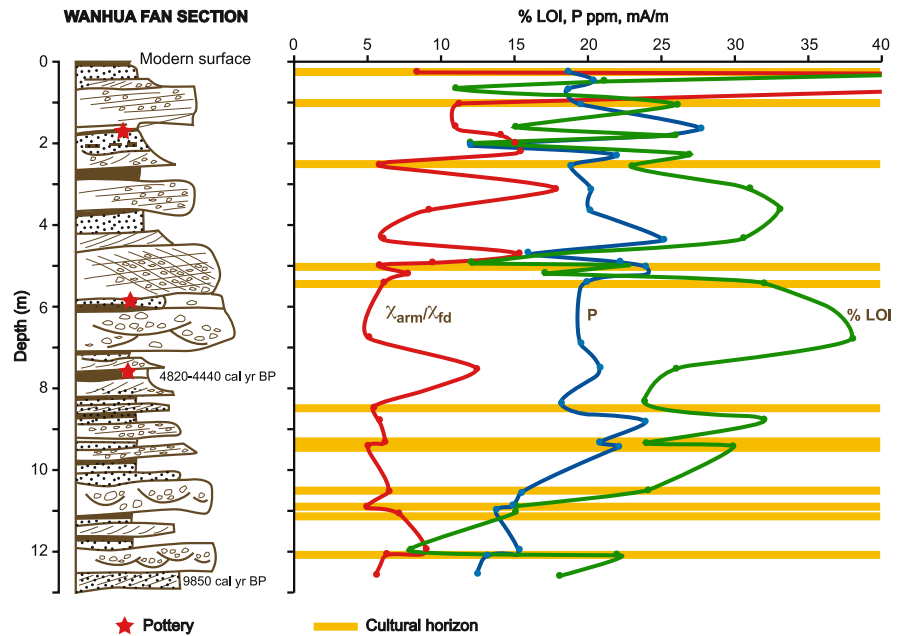
climate in Yunnan became warmer after the last glaciation (Walker 1986), with the Holocene optimum recorded at 7,000–4,000 <sup>14</sup>C year BP (Sun et al.

1986). Geochemical studies of sediments from the Lakes Xingyun Hu and Qilu Hu in the central part of Yunnan also suggest that the summer monsoon was

**Table 2** Timeline of human activities in the Erhai catchment and region derived from archaeological and documentary sources

~ 500–200 cal year BP (CE 1450–1750)	Late Ming/early Qing crisis (Elvin et al. 2002)
~ 900–600 cal year BP (CE 937–1253)	Dali Kingdom (Elvin et al. 2002)
~ 1,400–1,000 cal year BP (CE 738–902)	Nanzhao Kingdom (Elvin et al. 2002)
~ 2,300–1,700 cal year BP	Han Dynasty (Elvin et al. 2002)
~ 3,000–2,500 cal year BP	Bronze Age (Institute of Archaeology, 1990)
~ 4,150 cal year BP	Neolithic finds (Lin et al. 1986)
~ 5,700 cal year BP (est. 5,000 <sup>14</sup> C year BP)	Sub-Neolithic corded-ware ceramics (this study)
9,900–9,570 cal year BP	Dated charcoal in early cultural layer (this study)

**Fig. 4** Wanhua alluvial fan section (~ 13 m high) showing 12 possible cultural horizons in stratigraphic section, locations of Neolithic pottery, two <sup>14</sup>C dates (charcoal) of 4,820–4,440 cal year BP and 9,840 cal year BP, and proxies for bacterial magnetite ( $\chi_{ARM}/\chi_{FD}$ : mA/m), total soil phosphorus (P ppm) and organic matter (loss on ignition [% LOI])



strong from 12,000 to 8,000 cal year BP, but weakened gradually in response to insolation forcing during the mid-to-late Holocene (Hodell et al. 1999).

Most recently, two speleothem records of  $\delta^{18}O$  from Dongge Cave (Dykoski et al. 2005; Wang et al. 2005) lying ~ 750 km E of Erhai (Fig. 1) confirm the peak monsoon intensity at ~ 10,000–8,000 cal year BP which gradually weakens through the Holocene, strengthening only in the last 1,000 years. The comparability of low frequency changes in the two independent records is good, and at least for the past 2,000–4,000 years the records follow the broad patterns seen in speleothems from as far apart as Beijing, Liaoning Province and Guangxi Province (Tan and Cai 2005). However, claims for high frequency changes (Wang et al. 2005) that describe

relatively dry periods (centred on 8,300, 7,200, 6,300, 5,500, 4,400, 2,700, 1,600 and 500 cal year BP) need to be considered with caution as they are not clearly reproduced in the adjacent section (Dykoski et al. 2005). Statistical calibrations (Johnson and Ingram 2004) on modern monitored data show that while  $\delta^{18}O$  values in southern and western China are most strongly correlated to the amount of precipitation, they are also weakly correlated to monthly temperatures. Indeed, Tan and Cai (2005) argue that the  $\delta^{18}O$  record from Beijing, which correlates reasonably well with Dongge Cave, mirrors the latest reconstructed northern hemisphere temperature curve (Moberg et al. 2005). Throughout the paper, we use the higher resolution series from Dongge Cave (Wang et al. 2005) to indicate a compounded climate signal for the Erhai region, but one dominantly driven

by the seasonal precipitation associated with the southwest summer monsoon.

No independent and continuous temperature series exist for the last 12,000 years in southwest China, but the pollen-based temperature reconstruction from Mt Luojie (alt. 3,800 m) in southern Sichuan (~300 km NE of Erhai; Fig. 1) covering the period 11,000–1,500 <sup>14</sup>C year BP (Wang et al. 1990) and the sea surface temperature record based on UK<sup>-37</sup> alkenones (Pelejero et al. 1999) from the South China Sea (Fig. 1) are used to constrain the low frequency variability in regional temperature. Both records show rising temperatures after 12,000 cal year BP, reaching a plateau of relatively stationary values from ~6,000 cal year onwards. The records contrast during the late Holocene with the marine record, showing a slight increase after 2,000 cal year BP, and the pollen-based record showing a temperature decline after ~4,000 <sup>14</sup>C year BP, although the pollen record is incomplete and probably prone to human factors after 3,000 <sup>14</sup>C year BP.

## Methods and techniques

The main source of palaeoenvironmental data is a 6.48 m sediment sequence of four overlapping cores (EH2) retrieved from the northern edge of the central basin in April 2001 using a UWITEC sampling system in a water depth of 10.8 m (Fig. 2). The lithology changes from dark grey silty-clay below 60 cm to yellowish brown clay above 60 cm, which merges into brownish red clay above 10 cm. A previous chronology constructed from eleven AMS <sup>14</sup>C dates from seven depths (Shen et al. 2006) has been supplemented with independent palaeomagnetic dates, AMS <sup>14</sup>C dates published by Hyodo et al. (1999) for cores ER3 and ER1, two further AMS <sup>14</sup>C dates from an adjacent lake sediment core to EH2, and a catchment-wide stratigraphic boundary observed in a floodplain core in the river Miju delta (Fig. 2). All the extra <sup>14</sup>C dates were measured on charcoal, terrestrial macrofossils/wood, terrestrial shells or alkali insoluble fractions. The dates have been transferred to EH2 using core correlations based on magnetic parameters (Table 3). Xu and Zheng (2003) and Shen et al. (2006) discuss in detail the sources of error in <sup>14</sup>C dating of Erhai sediments, for example, that humic acid and terrestrial macrofossil ages are similar in the upper 70 cm but diverge by

more than 1,000 years in older sediments (Xu and Zheng 2003). But all evidence points to acceptably coherent dates derived from terrestrial macrofossils except where they are derived from old organic deposits. Comparisons of sediment ages at similar depths in the enlarged dataset suggests that only the 6,133 cal year BP date is significantly too old, possibly as a result of inwashed organic deposits.

Therefore a new depth-age curve (Fig. 5), utilizing the second-order polynomial ( $y = -0.0104x^2 + 25.331x - 25$ ;  $R^2 = 0.9828$ ), excludes this date. Measurement errors (2 sd) for the conventional AMS ages range from  $\pm 80$  year to  $\pm 170$  year, and an arbitrary value of  $\pm 100$  is assumed in discussions below. The 6.48 m sediment sequence stretches back from -25 (CE 1975) to 12,011 cal year BP, the polynomial describing a wet accumulation rate that increases with age from ~0.4 mm/year at the present time to 0.8 mm/year in the early Holocene, with a mean rate of ~0.54 mm/year (Fig. 4). Thus each centimetre sample represents 25–12 years and a century is represented by 4–8 cm. While the polynomial curve is appropriate for describing millennial scale changes, it should be noted that there are apparently significant higher frequency increases in sedimentation at ~5,000 and ~2,300 cal year BP.

Analysis of pollen, particle-size (laser granulometer), geochemistry (wet digestion, XRF, ICP-AES), stable carbon isotopes, and mineral magnetism follow standard procedures on 1 or 2 cm sediment subsamples. Specific details of the analyses and interpretation of the proxies are dealt with by Shen et al. (2005, 2006). A minimum of 300 pollen were counted, excluding Pteridophytes, Cyperaceae and aquatic taxa, and identified with guides compiled by the Institute of Botany, CAS (1960, 1976), the Institute of Botany, South China Institute of Botany, CAS (1982), and Wang et al. (1995).

The sediment geochemical data are interpreted in terms of compositional end members. Relative proportions of calcite, kaolinite, chlorite, and plagioclase minerals, and an assemblage of minerals that constitutes basalt rock, were determined by a combination of regression analysis and normative mineral calculations (Boyle 2001). Pollutant contributions to heavy metal concentrations were determined using a modified Hilton procedure (Boyle 2001), with Pb and Cu concentrations above background used as proxies for heavy metal extractive industries.

**Table 3** Mean cal year BP age ranges (all  $^{14}\text{C}$  AMS) and palaeomagnetic ages used to date EH2 showing source of date and means of correlation

EH2 depth (cm)	Mean age (cal year BP)	Source of date/correlation
0	-25	Authors' unpublished $^{210}\text{Pb}$ dated EH3/ $\chi_{\text{If}}$
14	150	Palaeo feature b ER3, Hyodo et al. (1999)/ $\chi_{\text{If}}$
33	400	Palaeo feature b ER3, Hyodo et al. (1999)/ $\chi_{\text{If}}$
49	1,200	Palaeo feature c ER3, Hyodo et al. (1999)/ $\chi_{\text{If}}$
49	1,200	Palaeo feature g ER3, Hyodo et al. (1999)/ $\chi_{\text{If}}$
57	1,585	$^{14}\text{C}$ ER3, Hyodo et al. (1999)/ $\chi_{\text{ARM}}$
58	1,190	$^{14}\text{C}$ date from Miju section, Beta-190726/ $\chi_{\text{If}}$
60	1,845	$^{14}\text{C}$ EH2, Shen et al. (2006)
61	1,400	Palaeo feature g-d, Hyodo et al. (1999)/ $\chi_{\text{If}}$
62	1,950	$^{14}\text{C}$ date on adjacent core EH2a, Beta-196114/ $\chi_{\text{If}}$
67	1,950	Palaeo feature d, Hyodo et al. (1999)/ $\chi_{\text{If}}$
65	1,885	$^{14}\text{C}$ ER3, Hyodo et al. (1999)/ARM
71	2,050	Palaeo feature d, Hyodo et al. (1999)/ $\chi_{\text{If}}$
76	2,610	$^{14}\text{C}$ ER3, Hyodo et al. (1999)/ARM
118	2,725	$^{14}\text{C}$ EH2, Shen et al. (2006)
120	3,030	$^{14}\text{C}$ ER1, Hyodo et al. (1999)/ $\chi_{\text{If}}$
186	3,560	$^{14}\text{C}$ ER3, Hyodo et al. (1999)/ $\chi_{\text{If}}$
196	3,765	$^{14}\text{C}$ ER3, Hyodo et al. (1999)/ $\chi_{\text{If}}$
216	5,050	$^{14}\text{C}$ ER3, Hyodo et al. (1999)/ $\chi_{\text{If}}$
226	5,105	$^{14}\text{C}$ ER3, Hyodo et al. (1999)/ $\chi_{\text{If}}$
346	7,682	$^{14}\text{C}$ EH2, Shen et al. (2006)
466	9,930	$^{14}\text{C}$ EH2, Shen et al. (2006)
536	10,329	$^{14}\text{C}$ EH2, Shen et al. (2006)

$2\sigma$  measurement errors on conventional radiocarbon ages are  $\pm 80$  to  $\pm 170$ . EH3, ER3, EH2a and ER1 are codes for other cores. Symbols b,  $\beta$ , c,  $\gamma$ ,  $\gamma$ - $\delta$ , d and  $\delta$  refer to declination and inclination features recorded in ER3 and dated by comparison with Chinese archaeomagnetic series reconstructed from pottery. Inter-core correlations through measurements of anhysteretic remanent magnetisation ( $\chi_{\text{ARM}}$ ) and magnetic susceptibility ( $\chi_{\text{If}}$ )

Magnetic susceptibility ( $\chi_{\text{If}}$ ) is used as a general proxy for silts/fine sands containing primary magnetite eroded from highly magnetic sources (e.g. basalts) through slope processes, such as gullyng. The percentage frequency dependent susceptibility ( $\chi_{\text{fd}}\%$ ) is used as a proxy for the relative contribution of surface erosion of clays and silts from well-developed low-mid altitude soil profiles (Dearing 1999). These detrital sediment-source linkages are based on magnetic analyses of  $\sim 160$  samples taken from soil profiles in the catchment.

Comparison of  $\sim 1$  m long sediment sequences along a transect between the core site and the Miju inflow (a distance of  $>5$  km) shows good correlations in geochemical and magnetic data for relatively coarse-grained detrital minerogenic sediment, but with the magnitude of values declining with

increasing distance away from the Miju river. Therefore, the sand ( $\% >63\ \mu\text{m}$ ) component of the sediments is used as a simple proxy of high fluvial energies bringing relatively coarse-grained sediment to the profundal lake area during floods associated with the peak monsoon period. Throughout the paper, dates are expressed as either calibrated radiocarbon years (cal year BP), uncalibrated radiocarbon years ( $^{14}\text{C}$  BP), or CE/BCE (Christian era/before Christian era) for archaeological and documentary records.

### Lake level changes—tectonics, climate or human controls?

One issue at Erhai concerns the history and causes of lake level fluctuations. Changes in lake levels may

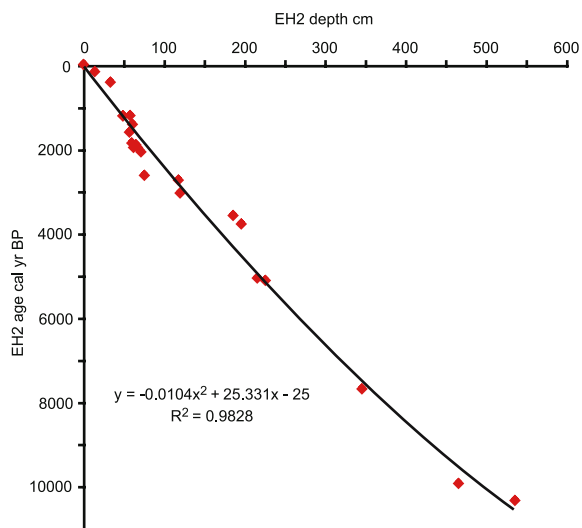


**Fig. 5** EH2 depth-age curve showing all actual  $^{14}\text{C}$  dates in EH2 (excluding 6,133 cal year BP), transferred  $^{14}\text{C}$  dates and palaeomagnetic ages from ER3 (Table 2 and Hyodo et al. 1999) and best-fit second order polynomial

provide information about water balances, but it is also necessary to identify the constraints that fluctuations in lake level/volume place on interpreting the lake sediment records in terms of changes to the lake and catchment systems. As in many lakes, it is an issue of disentangling the relative importance of tectonics, climate, human activities and natural infilling on lake elevation, lake margins and water depths (Dearing 1997).

### Tectonic controls

The basin is situated within the Dali fault zone that merges with the northern end of the Red River fault (Allen et al. 1984; Socquet and Pubellier 2005). Dominant lines of normal faulting with easterly dips along the western and eastern edges of the lake have, according to the latest studies (Wang 1998; Socquet and Pubellier 2005), led to basin subsidence and exhumation of the Diancangshan mountain range. As a result, the Erhai basin has accumulated an estimated 2,000 m of sediments during the Pleistocene (Wang 1998). The westerly mountain scarp extends northwards into the Dengchuan and Eryuan valleys, and is characterised by abrupt topographic transitions between the mountains and alluvial plains along the whole length, and by a  $\sim 18.8$  m deep trench

(Sun et al. 1999) close to the SW shore of Erhai. Recent faulting is evident from discontinuous fault scarps cutting the alluvial fans, numerous ‘Y-shaped’ valleys, young alluvial cones (Allen et al. 1984) and the many documented landslides and earthquakes. In CE 1925, Dali experienced an earthquake  $>7.5$  Richter scale, and at least 10 earthquakes  $>6$  Richter scale have occurred in the catchment (Fig. 3) since CE 780 (Allen et al. 1984).

Published data for cores taken from 2 to 10 km beyond the southern lake shoreline provide a record of relative lake elevation above the present water level. They suggest a late-Pleistocene lake level of  $\sim +26$  m at  $\sim 34,090 \pm 3,800$  year BP, relatively reduced levels of  $+21$  to  $+10$  m during the period  $23,050 \pm 1,300$ – $21,650 \pm 830$  year BP, and renewed high levels of  $+25$  m at  $18,700 \pm 560$  year BP to  $17,030 \pm 510$  and  $+33$  m at  $11,610 \pm 300$  year BP (Yu et al. 2001). There is also evidence from dated shell deposits near the lake shore of slightly higher lake levels ( $+1$  to  $+3$  m) at  $470 \pm 150$  year BP and at  $2,230 \pm 90$  to  $1,250 \pm 80$  year BP (Yu et al. 2001). The changes in lake level on the east shoreline have been far less, with little change since the late-Pleistocene (Zhu 1989). Our field observations of contacts between reclaimed lake bed and in situ deeply weathered slope profiles suggest that the modern lake level on the north-eastern shore is only a few metres ( $<10$  m) below an old, but undated, maximum high stand. Thus the highly contrasting evidence for lake fluctuations on different sides of the lake confirms that the first order control on lake elevation and position is tectonic. This agrees with geological evidence that the east shore and the lake basin are part of a subsiding block, delimited on the eastern side by a normal fault that runs 2–3 km inland of the lake (Socquet and Pubellier 2005), and on the western and northern margins by the Dali fault system (Guodong et al. 2001).

A lake margin elevation of  $+33$  m above present in the early Holocene implies that the Dali plain has gradually widened at a rate of  $\sim 2$ – $3$  mm/year, and also that Erhai has never fully inundated the northern Dengchuan basin. Early documented history identifies and confirms some of these dates and past locations of lake margins. Human clearance of extensive swamp forest growing on sediments along the western edge of the lake exposed by a receding lake margin probably occurred no later than

~3,000 cal year BP (Elvin et al. 2002). Establishment of the early Dali city and the construction of a 16 km long irrigation channel took place CE 738–845, confirming that the lake margin was clearly well down-slope of Dali at CE 900. Various pictorial maps from the Ming period also show the edge of the city set several kilometres from the shore. During the past millennium, the plain to the north of Dengchuan was described as covered with ‘sediments and muds’ with two small lakes draining into the Miju and Luoshi rivers, the latter an artificial channel excavated sometime between CE 581 and 1367 to improve drainage to the lake (Elvin et al. 2002).

### Human, climate and infilling controls

One potential control on actual water depth is human modification of the lake threshold in the Xier valley, a few kilometres downstream of Xiaguan and Erhai (Fig. 2). Here, the Xier river follows the normal fault that delimits the southern extent of the Diancangshan block (Socquet and Pubellier 2005), and currently flows through a small gorge (~10 m deep × 20–30 m long × ~4 m wide) artificially cut into a rock bar. The elevation of the modern low flow is ~29 m below the modern lake level but is controlled by a hydro-electric power station (built 1970s) just upstream of the gorge. Therefore we may assume that the threshold control on lake level has not been at this point since the lake was at least ~30 m higher than today, in the early Holocene. This means that we can exclude recent modifications to the rock bar as these would have only affected the river flow downstream of the lake, not the level of Erhai itself.

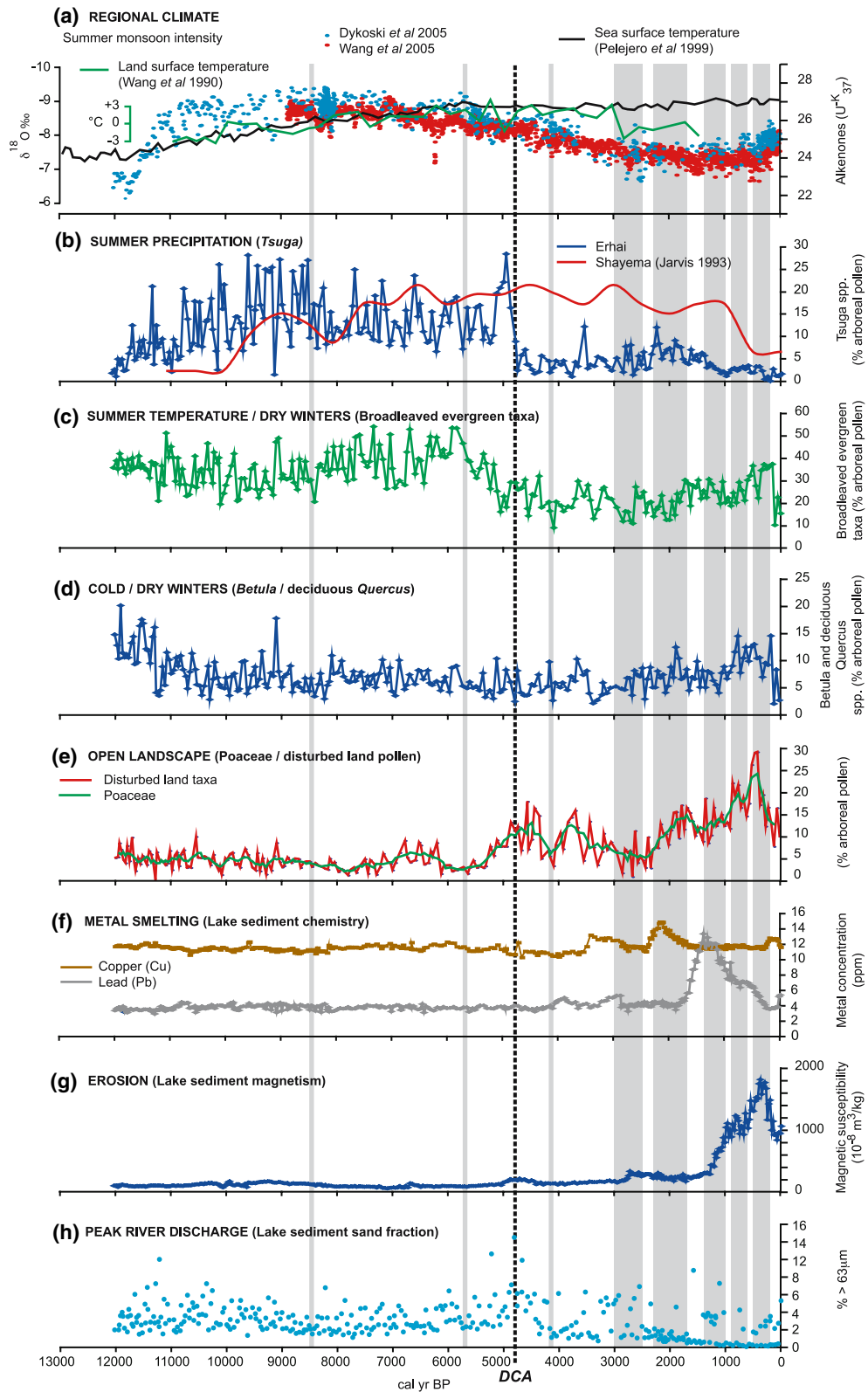
The lake volume has decreased during the Holocene due to lake infilling. With at least 5 m of Holocene sediment accumulation, it may be expected that the early Holocene mean water depth was significantly greater. A decreasing water residence time (currently ~2.5 years) would reduce the flux of suspended detrital and autochthonous organic particles in the water column to the lake surface. This effect seems to be confirmed by the declining rate of sediment accumulation (Fig. 5) through the Holocene, although this explanation has to be balanced with the effect of increased sediment storage in the catchment brought about by the natural enlargement of the Dali plain and widespread hydraulic modification.

Erhai is an open basin with a catchment: lake ratio of ~15 generating at the present time a large outflow volume (monitored at  $4\text{--}12 \times 10^8 \text{ m}^3/\text{year}$ : 1952–1974) equivalent to 66–88% of total inflow. As noted above, there may have been several regional dry phases through the Holocene (Wang et al. 2005) and certainly many recorded droughts (Elvin et al. 2002). However, it is difficult to envisage centennial-long stands of reduced water depths, with no running outflow, corresponding to these times. Similarly, higher outflow levels caused by periods of reduced evapotranspiration or strengthened monsoonal activity would also be accommodated by the outflow and would be expected to increase seasonal water depths by 1–2 m at most. Thus, corroborating evidence for perennial climate controls on water depth is weak. If the lake has experienced short term fluctuations in water depth fluctuations, the more likely cause is tectonic activity affecting outflow elevation and basin leakage. On the basis of this evidence, it is assumed that lake sediment records from the central lake zone provide acceptably coherent records of catchment vegetation and fluvial responses through the Holocene.

### Millennial-scale environmental changes—climate and human controls

Disentangling the roles of climate and human activities on sediment records of environmental conditions and processes is facilitated by the use of independent time series drawn from different archives. Here, we assess millennial-scale interactions by analysing the apparent connections between the independent regional climate signals (Fig. 6a), inferred local vegetation responses (Fig. 6b–d), land use changes (Fig. 6e), metal workings (Fig. 6f), erosion and fluvial records (Fig. 6g and h), and the independently recorded human activities (Table 2).

The lake pollen record shows *Betula* and deciduous *Quercus* (Fig. 6d) dominating between 12,000 and 11,000 cal year BP, in line with the expected response to independent climate series that show cold temperatures and relatively dry conditions associated with the end of the Younger Dryas and early Holocene (winter mean temperatures in southwest China as low as  $-10 \text{ }^\circ\text{C}$  with 500–600 mm annual precipitation: Jarvis 1993). *Tsuga* also tolerates cold



◀ **Fig. 6** Millennial-scale climate–human–environment interactions (13,000–0 cal year BP): (a) regional climate proxies comprising summer monsoon intensity proxies from oxygen isotope analyses of speleothems at Dongge Cave (Wang et al. 2005; Dykoski et al. 2005), pollen-based temperatures from Mt Loujie, southern Sichuan province (Wang et al. 1990), and sea surface temperature curve for the South China Sea based on alkenone analysis of marine core 17,940 (Pelejero et al. 1999); (b) Erhai lake sediment *Tsuga* pollen curve associated with high summer precipitation, with *Tsuga* curve from Lake Shayema (Jarvis 1993); (c) Erhai lake sediment broadleaved evergreen pollen curve associated with high summer temperatures/dry winters; (d) Erhai lake sediment *Betula* plus deciduous *Quercus* pollen curves associated with cold/dry winters; (e) Erhai lake sediment Poaceae and disturbed land pollen taxa curves associated with open/agricultural landscapes; (f) Erhai lake sediment copper and lead curves (with background values removed) used as metal smelting proxies; (g) Erhai lake sediment magnetic susceptibility curve used as an erosion proxy [ $\chi_{lf}$ ]; (h) Erhai lake sediment sand fraction (% >63  $\mu\text{m}$ ) date used as proxy for size of floods. Vertical dotted line denotes the major shift in pollen assemblage determined by DCA (Shen et al. 2006) at  $\sim 4,860$  cal year BP. Vertical shaded bars define main periods of human occupation recorded in archaeological/historical records (Table 2)

conditions but is susceptible to drought, requiring annual precipitation values of 1,000–1,500 mm (Jarvis 1993). The rise in *Tsuga* from 12,000 cal year BP, reaching a peak  $\sim 9,500$ – $8,500$  BP (Fig. 6b), is therefore also broadly consistent with the strengthening monsoon, while the decline in *Betula* and deciduous *Quercus* is consistent with increasing temperature. Since broadleaved evergreen taxa are indicative of high summer temperatures and dry winters, the stationary values for these taxa (Fig. 6c) before  $\sim 8,000$  cal year BP confirm that the main climatic drivers of change in the early Holocene were increasing summer monsoonal precipitation and increasing winter temperature.

The period 8,500–6,000 cal year BP signifies a change in the climate. Reduced *Tsuga* and enhanced broadleaved evergreen forest suggest that there was a shift to greater seasonality at this time: warmer and drier summers with drier, and from the minor recovery in the *Betula* and deciduous *Quercus* curve, colder winters. Very similar biotic responses are recorded at Lake Shayema (Jarvis 1993) in southwest Sichuan (2,400 m a.s.l. and  $\sim 400$  km northeast of Erhai). Similarly, the pollen indicators of dry valley habitats (Euphorbiaceae and *Eomecon*) are high throughout the period up to  $\sim 6,000$  cal year BP (Shen et al. 2006), consistent with a weakening or failure of the winter frontal systems.

The effects of these climate changes are also seen in the lake sediment proxy for river discharge which broadly describes the trend and variations in the size of large floods (Fig. 6h). Between 12,000 and 10,000 cal year BP the trend broadly follows the strengthening monsoon and warming curve, but then the envelope of points reduce until  $\sim 8,000$  cal year BP. This probably reflects both the impact of increasing vegetation cover and soil maturation which gradually moderated flood levels, and the diminishing role of spring snowmelt after 10,000 cal year BP as winters became warmer. Following the peak summer monsoonal intensity  $\sim 8,000$ – $6,000$  cal year BP, the river flooding record shows increasing variance that may reflect the increased climate seasonality, including greater snow cover.

The temperature optimum at 7,000–5,000 cal year BP is a period when the monsoon intensity is weakening. At  $\sim 6,000$  cal year BP, broadleaved evergreen forest begins to decline, followed by declines in dry valley species (Shen et al. 2006) and eventually *Tsuga* ( $\sim 4,800$  cal year BP). Explanations for the dramatic declines in broadleaved evergreen forest and *Tsuga* could be nonlinear responses to gradually changing climatic conditions. However, there are three reasons to suggest that these changes are not solely the result of climate.

- (1) Detrended correspondence analysis (DCA) of the pollen data (Shen et al. 2006) shows that the most significant shift in the whole pollen assemblage is linked to the mid-Holocene rise of open landscape/disturbed taxa indicative of major human activity, dated to  $\sim 4,900$ – $4,800$  cal year BP (dotted line in Fig. 6).
- (2) The curves for *Tsuga* and evergreen sclerophyllous taxa at the small and remote site of Lake Shayema (Jarvis 1993) are similar both before and after this shift (Fig. 6b), declining only in the last 1,000 ( $^{14}\text{C}$ ) years as a result of late human activity.
- (3) The percentage aquatic pollen curve (Shen et al. 2006) rises strongly after 5,000 cal year BP suggesting an increased area of open wetland or shallow lake environments more plausibly attributed to human manipulation of catchment hydrology than a weakening monsoon climate.

To what extent can the various trends and fluctuations in the sediment proxy records after 5,000 cal

year BP be used as response signals to climate and human activity? It might be expected that the aggregated pollen curves (Fig. 6e) for taxa indicative of open/disturbed landscapes (Poaceae, Compositae, *Artemisia*, *Plantago* and Chenopodiaceae) generally, and Poaceae, specifically, may be used as a proxy for agricultural activities. The curve describes three millennial-scale periods of landscape change increasing in either extent or intensity towards the present ( $\sim 7,500$ – $6,000$  cal year BP;  $\sim 5,300$ – $2,750$  cal year BP, and  $\sim 2,500$  cal year to present) but only the last period closely tracks the historical recorded phases of human activity from the Han Dynasty to the Ming/Qing crisis. The historical evidence for the earlier periods of apparent land disturbance is far weaker. However, all three periods of disturbance are linked to evidence for enhanced erosion and sediment transport, as shown by peaks in the magnetite ( $\chi_{lf}$ ) proxy for erosion (Fig. 6g), which may indicate soil disturbance. In this context, the magnetic erosion proxy provides a compound indicator of deposited silt and fine sands derived from mainly igneous and metamorphic sources (Dearing 1999). The first period is linked to a small erosion peak, lying just outside the background variance, but the second and third periods form part of a stepped and increasing trend in erosion that starts in the Neolithic, steps up in the Bronze Age before accelerating through the time of the Nanzhou and Dali Kingdoms, and reaches a peak during the documented late Ming/early Qing crisis. Actual increases in sediment transport during the early periods of land disturbance are also suggested by relatively rapid rises in the lake sedimentation rate at  $\sim 5,000$  and  $2,300$  cal year BP (Fig. 5).

The proxy for Cu smelting (Fig. 6f) shows three distinct peaks starting  $\sim 3,400$ ,  $2,200$  and  $180$  cal year BP, the first two corresponding to the documented early and peak usage of bronze. The earliest bronze culture in the area is described from Jianchuan to the north of Erhai (Fig. 1), where bronze axes, sickles, fishhooks, bracelets and ornaments are dated to  $\sim 3,300$  cal year BP (Institute of Archaeology, Yunnan Province 1990). Copper is also reported to have been in use in the Erhai area by  $\sim 3,000$  cal year BP (Lin et al. 1986), and by  $2,800$  cal year BP the Kunming had established an extensive bronze culture in the wider Erhai region (Zhang 1990). In contrast, high values in the curve for Pb, a by-product of silver smelting, cover the period  $1,600$ – $250$  cal

year BP with a peak  $1,400$ – $1,000$  cal year BP. Dali has been one of the foremost silver-producing areas in Yunnan, with numerous mines in the Diancangshan mountains. Documentary evidence points to an upsurge in silver production in the catchment sometime before CE 700, a maximum in the period  $\sim$ CE 800–1200, followed by a decline to the point of eventual non-existence CE 1700–1900. Thus, within the dating uncertainties the sediment proxies for metal workings match the documentary evidence well. Interestingly, neither the Cu nor Pb curves are in phase with the erosion curve, suggesting that mining was localised in its operation and effect.

The periods of open/disturbed landscape may also be linked to the trend and variance of river discharge (Fig. 6h). The first coincides with a small rise in discharge variance that has also been attributed to increased climate seasonality. The second is initially linked to the phase of increased discharge variance that peaks around the major pollen shift (DCA) but then the association breaks down with high levels of disturbance linked to a reducing trend of river discharge. The third period is also linked to a declining trend in river discharge but with occasionally high discharge variance. This starts  $\sim 2,500$  cal year BP and continues through the next two millennia of documented human activities, until a small upturn  $\sim 500$  cal year BP. On the one hand, these millennial trends in river discharge appear to track partially the weakening monsoon record (Fig. 6a). But on the other hand, the argument could be made that land management after  $\sim 5,000$  cal year BP, created a hydraulic and hydrological system that has suppressed flood peaks. Overall the evidence for using the open/disturbance taxa, and metal records, as useful first order measures of the timing of human impact over millennial timescales is strong, particularly since  $\sim 5,000$  cal year BP. Moreover, we would argue that on millennial timescales the timing and length of these disturbance phases are not in phase with the trends or fluctuations in temperature or precipitation. The closer links with proxy records of erosion and, to a lesser extent, flooding suggest possible major modification of catchment processes by human activities.

Thus millennial-scale climate–human–environment interactions through the Holocene are divided into four phases: an early phase before  $\sim 8,000$  cal year BP when the ameliorating Holocene climate

operated as the first order control on vegetation establishment and development; a second phase  $\sim 8,000$ – $6,000$  cal year BP when climate seasonality played an important role in determining vegetation and river discharge, and when there may have been the first signs of significant human impact; a third phase  $\sim 6,000$ – $5,000$  cal year BP when human activity began to exert a measurable effect on local environmental processes; and a final phase after  $\sim 5,000$  cal year BP when human activity displaced climate as the first order control on trends in vegetation, erosion and, possibly, hydrology. The following sections consider the human–climate–environment interactions in more detail and at sub-millennial scales through three consecutive periods of increased open/disturbed landscape: the earliest agriculture (7,500–5,000 cal year BP); mid-Holocene deforestation (5,000–2,500 cal year BP); and recent urbanisation and population growth (post 2,500 cal year BP).

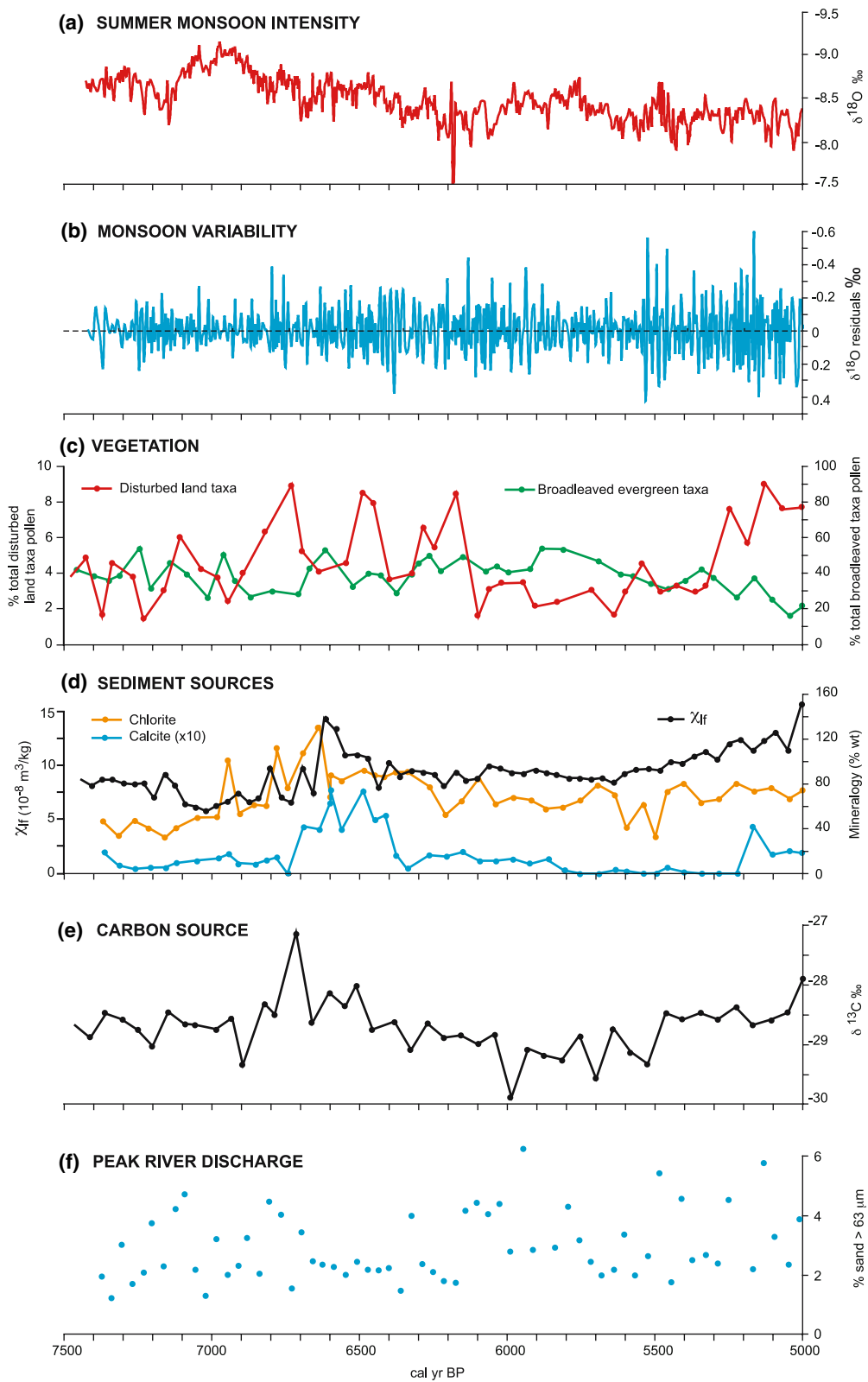
### Earliest agriculture (7,500–5,000 cal year BP)

The monsoon record during this period begins strong prior to  $\sim 6,800$  cal year BP before weakening and settling into a fairly stable and stationary trend (Fig. 7a). The disturbed land pollen taxa curve identifies two periods of disturbance during this period:  $\sim 7,000$ – $6,200$  cal year BP and from 5,400 cal year BP (Fig. 7c). The first phase is strongly linked to a reduction in arboreal pollen, particularly *Pinus* (Shen et al. 2006), rather than broadleaved evergreen forest taxa (Fig. 7c). Concentrations of chlorite, magnetite (Fig. 7d) and plagioclase also rise at this time though with a measurable time-lag of  $\sim 100$  years after the initial rise in disturbance taxa. Synchronous peak values for these minerals and rock types indicate metamorphic sources, as found in the western Diancangshan mountains (Fig. 3). There is also an increase in calcite (Fig. 7d) that co-varies with a shift towards less negative  $\delta^{13}\text{C}$  values (Fig. 7e). Dali limestone has a  $\delta^{13}\text{C}$  value of 0‰ (Chen et al. 2005), suggesting that a significant part of the calcite is detrital, originating in the metamorphic Diancangshan range. The climate at that time was characterised by peak Holocene temperatures and the beginning of the long term weakening of the monsoon (Fig. 7a), which

together might register the onset of warmer summers and drier/cooler winters, but there are no obvious links between the fluctuations in monsoon variability and the timing of disturbance (Fig. 7b). The high values for river discharge before the first disturbance phase appear to be coupled with the peak monsoon intensity centred on  $\sim 7,000$  cal year BP (Fig. 7a).

The second phase of apparent human impact after 5,400 cal year BP describes the beginning of the long-term decline in broadleaved evergreen forest (Figs. 6c and 7c). This decline is associated with gradually rising values in disturbed land taxa and sediment sources within the metamorphic zone, but despite higher monsoon variability there are only slight changes in the river discharge record. Taken together, the evidence for this period identifies human impacts largely in terms of vegetation change on the western mountains and plain, with the possible effect of increasing fluvial sediment transport.

What do archaeological and documentary records offer to help clarify these reconstructions? Neolithic remains have previously been recorded from alluvial fans at the base of the Diancangshan mountains adjacent to the lake, and culturally similar materials with rice at nearby Baiyangcun have been dated (Lin et al. 1986) to 3,770  $^{14}\text{C}$  year BP ( $\sim 4,150$  cal year BP). But this date for the earliest recorded human activities is nearly three millennia *later* than the sediment-based pollen evidence for early human impact shown in Fig. 7. Only the studies on the Wanhua alluvial fan (Fig. 4) corroborate the view that some form of local, sedentary agriculture existed well before 5,000 cal year BP, and provide evidence for some form of agriculture having been practised as far back as 9,000 cal year BP. Indeed, analysis of the magnetic and geochemical properties of the fan section (Fig. 4) may even provide insight into the early use of irrigation. The ratio of anhysteretic remanent magnetization ( $\chi_{\text{arm}}$ ) to frequency dependent susceptibility ( $\chi_{\text{fd}}$ ), an index of the ratio of stable single domain to superparamagnetic magnetite, rises to the surface as would be expected if there were an increase in waterlogging or the growth of microaerobic magnetotactic bacteria resulting in a relative reduction of ultrafine pedogenic iron oxides in the soil (e.g. Dearing et al. 2001). Together with the high levels of preserved organic matter, these lines of evidence allow speculation that the growth of irrigation (as frequency or increased water volumes), as



◀ **Fig. 7** Centennial-scale climate–human–environment interactions 7,500–5,000 cal year BP: (a) summer monsoon proxy (speleothem oxygen isotopes) (Wang et al. 2005); (b) monsoon variability (detrended curve (a)); (c) vegetation (broadleaved evergreen pollen taxa, disturbed land pollen taxa); (d) sediment source proxies (lake sediment magnetic susceptibility [ $\chi_{lf}$ ], chlorite and calcite mineralogies); (e) carbon source proxy (lake sediment  $\delta^{13}\text{C}$ ); (f) peak river discharge proxy (lake sediment sand fraction)

practised on the modern fan surface, started in the mid-Holocene.

Thus earliest human impacts on environmental processes are defined by vegetation clearance on the lower western slopes, presumably by a combination of deforestation, burning and grazing, and the disturbance of detrital sediment sources; though tectonic activity triggering landslides and fluvial adjustment cannot be ruled out. Subsequent impacts included the beginning of the deforestation of broadleaved evergreen forest along the shoreline, but these too had few impacts on catchment hydrology. This was possibly a period of greater seasonality in climate with winters becoming drier and cooler, but the proximity to permanent rivers flowing off the mountains would have offset any threat of perennial drought conditions: there is no evidence to suggest that human activities in the first half of the Holocene were directly determined by climate variations.

### Mid-Holocene deforestation (5,000–2,500 cal year BP)

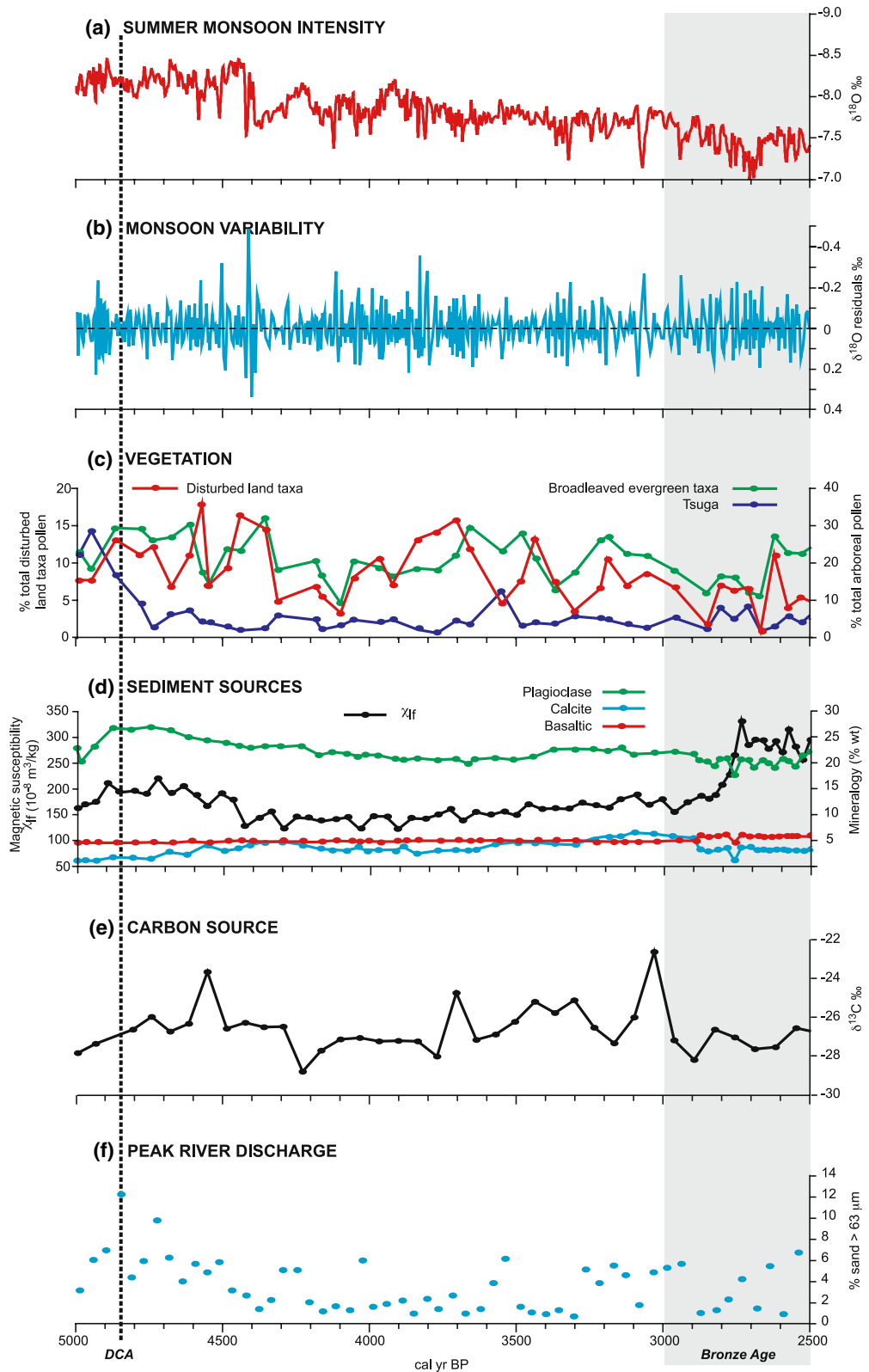
The monsoon record during this period is characterised by a gradual weakening, with a significant change in the isotope concentrations at  $\sim 4,400$  cal year BP interpreted elsewhere as a major drought period (Wang et al. 2005). The pollen records show that this period is characterised from the DCA defined shift at  $\sim 4,900$ – $4,800$  cal year BP by an overall expansion of open/disturbed land at the expense of initially *Tsuga* (4,900–4,400 cal year BP) and then lowland broadleaved evergreen forest (Fig. 8c). There are two phases of high values of open/disturbance taxa at 4,900–4,400 cal year BP and 3,900–3,400 cal year BP.

The first phase is associated with a major decline in *Tsuga* that typically grows on mid-high mountain slopes (2,250–3,750 m: Lin et al. 1986). This loss of a forest species is associated with expansion of

disturbed pollen taxa and increased variance in the river discharge proxy (Fig. 8f), representing the first significant increase in river discharge that does not appear to track the monsoon trend (Fig. 8a) or decadal variability (Fig. 8b). The implications are that upland deforestation led to increased areas of pasture and short term levels of enhanced runoff. Lagged peaks in levels of transported plagioclase, magnetite, calcite (Fig. 8d) and Dali marble (Fig. 8e) at this time indicate increased delivery of sediments from the Diancangshan mountains. In contrast, the second disturbance phase is linked to only minor changes in river discharge and erosion proxies suggesting that deforestation was restricted at low altitudes.

Towards the end of the period, from  $\sim 2,800$  cal year BP, there are sharp increases in erosion proxies, particularly the magnetic and geochemical evidence for the beginning of sediment delivery from basalt rock sources (Fig. 8d), but these are associated only with declines in broadleaved evergreen taxa with no clear increase in disturbed land taxa. Basalt regoliths and soils dominate the northeastern slopes adjacent to the lake and Dengchuan valley, and the western slopes of the Dengchuan and Eryuan valleys (Figs. 2 and 3), but also underlie the floodplain deposits at the southern end of the Miju valley (our field inspections). A flux of basalt material could therefore signify either cultivation on the steep valley slopes or early attempts to artificially drain and dyke the wet valley floors. Given the evidence for broadleaved forest clearance it seems more likely that the sharp change in sediment geochemistry at  $\sim 2,900$ – $2,700$  cal year BP registers the start of the drainage of the northerly river valleys. A further line of evidence is the coincident stabilization of  $\delta^{13}\text{C}$  values at around  $-26.5\text{‰}$  which remain unvarying, by comparison with less negative peaks earlier in the record, up to the present day. These are very similar values to those measured on other recent Erhai sediments by Whitmore et al. (unpublished data) and are typical of terrestrial plant macrofossils.

Archaeological evidence (Zhang 1990) for agriculture during this period indicates that the Siyu and Kunming people, adopting a mixed herding and sedentary farming economy, had moved into the Erhai area by 3,200 cal year BP. Pastoralism in this part of Yunnan was certainly important for raising horses for export, from at least 2,600 cal year BP



◀**Fig. 8** Centennial-scale human–environment interactions 5,500–2,500 cal year BP: (a) summer monsoon proxy (speleothem oxygen isotopes) (Wang et al. 2005); (b) monsoon variability (detrended curve (a)); (c) vegetation (broadleaved evergreen pollen taxa, *Tsuga* pollen, disturbed land pollen taxa); (d) sediment source proxies (lake sediment magnetic susceptibility [ $\chi_{lf}$ ], plagioclase, calcite and basalt mineralogies); (e) carbon source proxy (lake sediment  $\delta^{13}\text{C}$ ); (f) peak river discharge proxy (lake sediment sand fraction). Vertical dotted line denotes the major shift in pollen assemblage determined by DCA. Vertical shaded bar defines main period of recorded human occupation (Table 2)

(Yang 2004b). The deforestation of high altitude *Tsuga* started  $\sim 1,500$  years earlier than these dates, but losses of broadleaved evergreen forest at lower altitudes continued throughout the period. One interpretation would be that the archaeological evidence describes the end of a gradual process through which sedentary agriculture and grassland extends into the lowland valleys. This is in accord with environmental history that places the clearance of the western Dali plain as occurring prior to 3,000 cal year BP (Elvin et al. 2002). At this time, the south-west Silk Road already ran close to the southern edge of Erhai (Fig. 1), and it is probable that population densities were higher in the southern and western parts of the catchment than the more isolated northerly basins (Yang 2004a).

At the end of the period there is sediment evidence for drainage activities in the northerly basin that could signify widespread attempts to irrigate the lowland valleys. While data from the Wanhua fan section suggests semi-continuous agricultural occupation since the early Holocene, with the possibility of localized irrigation since the mid-Holocene, there are as yet no direct archaeological records of irrigated farming in the valley bottoms. Outside the catchment, the Baiyangcun site (Fig. 1) that includes evidence of rice cultivation, is dated at  $\sim 4,150$  cal year BP. There, surveys suggest that houses were built with vertical posts and woven branches, daubed with mud and straw for the walls. It has been argued that the depth of the accumulated materials points to long periods of fixed residence, possibly sedentary growers of rice (Zhang 1990). On the basis of this date and others it has been suggested by Higham (2005) that there was a Neolithic wave of rice cultivation through southern China, inland along the main river valleys  $\sim 4,950$ – $3,950$  cal year BP though not necessarily resulting in extensive establishment. The first direct

evidence for paddy field cultivation at Erhai takes the form of a ceramic model showing an enclosed field and a pond, with a sluice-gate, channels, and domesticated animals, dated from the Han dynasty ( $\sim 2,300$ – $1,700$  cal year BP), found in a grave at the southern end of the lake (Elvin et al. 2002). Given the evidence for localized irrigation on fans, it is not unreasonable to suggest that irrigated farming was taking place in the valleys several centuries before this find, between 3,000 and 2,500 cal year BP. Indeed, there may be arguments to support this from further consideration of the climate record.

The whole of this period follows the long term weakening of the summer monsoon, including phases of higher monsoon variability at  $\sim 5,500$ ,  $\sim 4,400$  and  $\sim 3,800$  cal year BP (Fig. 8b). There are no obvious direct and linear links between either the monsoon trend or variance, and the timing of human activity. However, the high monsoon variability at  $\sim 4,400$  cal year BP (Fig. 8b) is followed by an extreme monsoon weakening: a dry and possibly cooler phase lasting  $\sim 500$  years that has been implicated in the cause of societal collapse in central and northern China and elsewhere (Wang et al. 2005). It is unlikely that a dry phase of this length and intensity would cause social collapse in a high altitude and mountainous, sub-tropical region, but it may have acted as a ‘stressor’ that drove agricultural innovation and the introduction of widespread irrigation. The justification for this argument lies in the fact that the underlying trend in river discharge decreases from this time while the maxima tend to increase in magnitude and frequency from  $\sim 4,400$  cal year BP onwards (Figs. 6h and 8f). This suggests both an enhancement of high flood maxima and suppression of low flood maxima. It would be difficult to explain the increase in maxima if these changes were solely driven by the long term weakening monsoon (Fig. 8a) because there are no clear links between monsoon variability (Fig. 8b) and the river discharge record (Fig. 8f). Thus, this apparently paradoxical observation is consistent with the gradual shift over centuries towards widespread irrigated land use at the same time as the monsoon weakens. Artificial ponds, bunds and paddy fields increase the water holding capacity of the catchment in normal conditions, and thus depress low discharge levels. But increased hydrological connectivity throughout the catchment, caused by hydraulic engineering of dykes,

canals and flood defences, accentuates river discharge levels under high magnitude-low frequency monsoon conditions.

### Urbanisation and population growth (since 2,500 cal year BP)

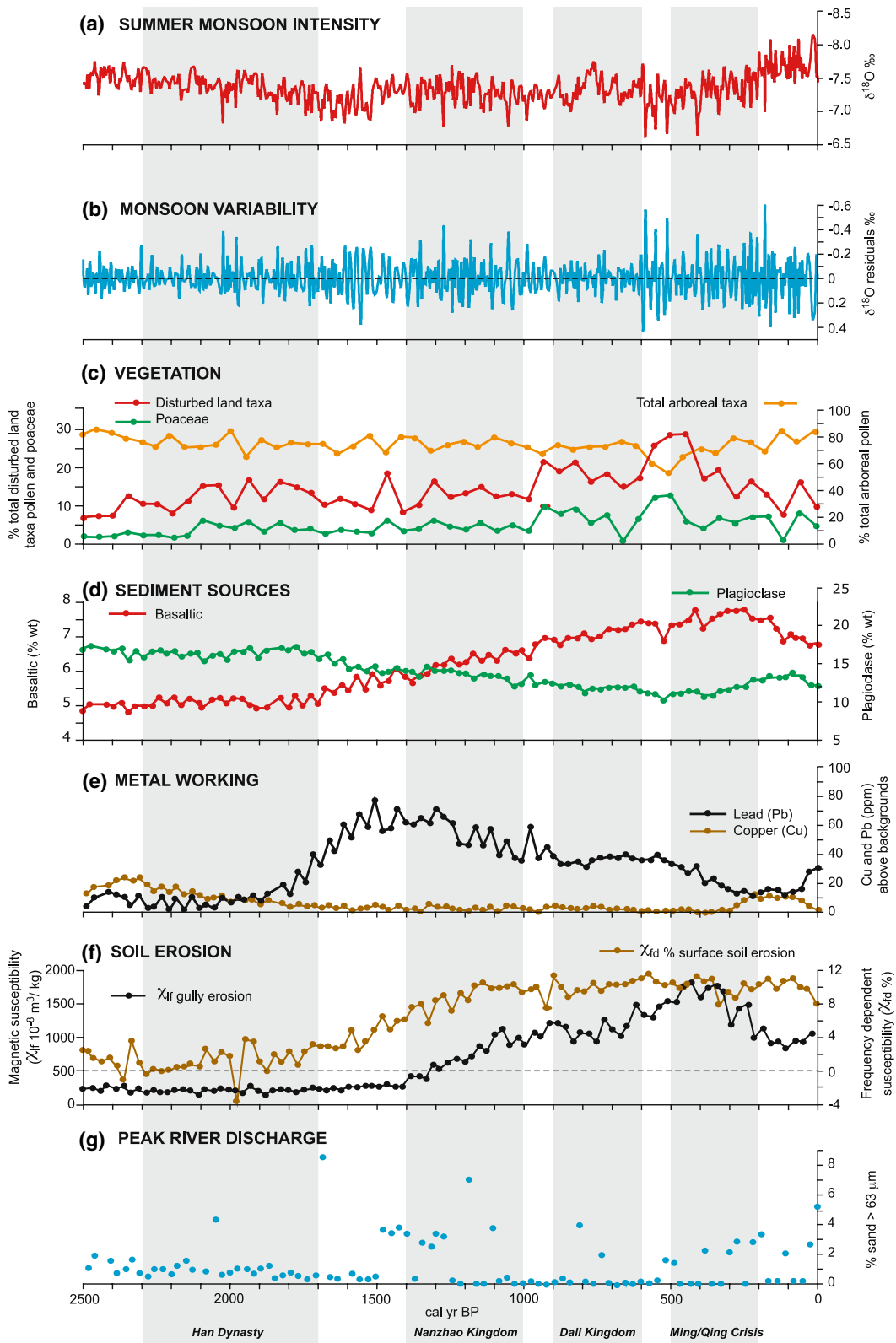
The monsoon record (Fig. 9a) during this period shows the end of the millennial scale weakening at  $\sim 1,400$  cal year BP, fluctuating over the next  $\sim 800$  years before showing a strong upward trend after 400 cal year BP. The pollen evidence defines four periods of vegetation disturbance: 2,000–1,600 cal year BP; 1,400–1,000 cal year BP; 900–600 cal year BP; and 500–150 cal year BP. Despite the sediment dating uncertainties, these map well onto the main historical recorded periods of human activity (Elvin et al. 2002): the inward migration and establishment of the Han Chinese (2,300–1,700 cal year BP); the rise and fall of the Nanzhao Kingdom (CE 738–902); the Dali Kingdom (CE 937–1253) and the environmental crisis in late Ming and Qing times (CE 1644–1911).

The decline in arboreal pollen from  $\sim 2,200$  cal year BP and the rise in open/disturbed land taxa, especially Poaceae, during the period 2,000–1,600 cal year BP (Fig. 9c) are most likely associated with the main Han influx. Hydraulic modification may have been practised earlier, but it is likely that this phase marks the widespread establishment of rice cultivation, terracing and paddy fields throughout the lower catchment. Geological sources of sediment remained more or less constant during the period, with an increase in basalt sediment and a decline in plagioclase occurring at the end of the phase  $\sim 1,700$  cal year BP (Fig. 9d) rather than during it. Climatically, the data suggest a continuing weakening of the monsoon with average to low levels of variability, but there is also no evidence for enhanced high flood maxima (Fig. 9g) caused by the disturbance. Together these lines of evidence strongly suggest that the impact of the Han was through extended use of irrigated farming in the northern basalt-rich valleys, which acted to suppress flood peaks. The Han were not hill-farmers and appear to have made little impact on slope processes. At the end of this phase, however, there is a significant rise in Pb accumulation (Fig. 9e) which signals the start

**Fig. 9** Centennial-scale human-environment interactions 2,500–0 cal year BP: (a) summer monsoon proxy (speleothem oxygen isotopes) (Wang et al. 2005); (b) monsoon variability (detrended curve (a)); (c) vegetation (total arboreal pollen, disturbed land pollen taxa, Poaceae pollen); (d) sediment source proxies (lake sediment plagioclase and basalt mineralogies); (e) metal working proxies (lake sediment copper and lead analyses with background values removed); (f) soil erosion and gully sediment source proxies (lake sediment frequency susceptibility [ $\chi_{fd}\%$ ] and magnetic susceptibility [ $\chi_{fd}$ ]); (g) peak river discharge proxy (lake sediment sand fraction). Vertical shaded bars define main periods of recorded human occupation (Table 2)

of substantial silver mining that peaked a few centuries later at the time of the Nanzhao/Dali Kingdoms (Fig. 9e).

The main sediment features of the second and third phases (1,400–1,000 cal year BP and 900–600 cal year BP) are the steady rise in topsoil erosion, and the rise and fall of silver workings. Our studies of  $\sim 160$  soil samples, show that frequency-dependent susceptibility ( $\chi_{FD}$ ) is diagnostic of pedogenic ferrimagnetic minerals that are found predominantly in well-drained surface soil (upper  $\sim 1$  m) horizons (Dearing et al. 1996, 2001). The start of the increase  $\sim 1,600$ –1,500 cal year BP (Fig. 9f) therefore marks a new environmental process operating in the catchment: significant surface erosional processes operating on lower and middle slopes, particularly the basalt and limestone formations. The co-variance with curves for the inorganic fraction (Shen et al. 2006), percentage clay and kaolinite (not shown) also strongly suggests that the dominant process is surface wash and rilling on exposed soil surfaces, as expected at the beginning of widespread rain-fed cultivation or overgrazing. The curves for magnetite-rich and basalt sediment sources rise more or less in parallel over the second and third phases, suggesting a common source in the northern catchment. The apparent time-lag between the topsoil and magnetite proxies is most easily explained by shallow erosion processes gradually triggering deeper gully erosion: a phenomenon that dominates the modern geomorphology over many of the slopes up to 2,500 m in the Dengshuan and Eryuan basins. Logically, gully development driven by rain-fed agriculture and overgrazing would be expected to enhance hydrological connectivity, runoff and hence extreme flood events. It is therefore noteworthy that the start of anomalously high flood maxima (Fig. 9g) at the beginning of the second



phase occurs at the same time as the magnetite proxy for gullying begins to rise.

By the time of the second and third phases, written records document the substantial levels to which the economy, urbanization, and population had already developed. For example, in CE 648, the Tang general Liang Jianfang described the Erhai region as “... containing several tens to a hundred tribes. ... They inhabit the mountains and [the banks of] rivers, and do not recognize any order of mutual subordination ... They have walled cities, suburbs [with outer walls], villages, and [fortified settlements]. ... Their lands have rice, wheat and barley, millet, and beans. Planting and harvesting are the same as in China. ... They raise cattle, horses, pigs, sheep, chickens, and dogs. ...” (quoted by Elvin et al. 2002). The exact extent of ‘the Erhai region’ is not clear but the figures suggest 160,000–480,000 people (cf. modern population 800,000). During the second phase, there is the first reference to direct drainage activities in the Dengshuan valley when the outflow of the West lake (Fig. 2) was re-routed directly to Erhai by cutting through the ridge to the south. Around CE 766, a stele in Nanzhao was set up by the officials to praise the leader’s achievements. “Walled cities and settlements stretched out one after another [while] villages were as dense as [the prongs on] a comb. He blocked off the currents and floods, so that the upland plains became fields for rice and millet. He drained and breached the pools and ponds, so that the low-lying wetlands could be properties planted with gardens and groves.” (quoted by Elvin et al. 2002). By CE 900 there is also direct evidence of substantial hydraulic engineering on the west shore of Erhai. In CE 845 the Army General Lord Sheng was sent to build the Transverse Channel to join together twelve of the streams for irrigation. He also created a water reservoir south of the summit of Yuju Peak in the Diancangshan range and directed mountain springs so that they drained off to flow as a river. Together it has been estimated that these actions enabled irrigation over ~54,000 ha in Tang times (CE 618–907) and 70,000 ha in the Ming (CE 1368–1644). Thus the establishment of irrigation in the first phase was now a dominant land use in the valleys and the Dali plain, and there is documented evidence to corroborate the sediment record that agriculture had moved into the ‘upland plains’ and mountains. The peak accumulation of Pb in the sediments ~1,400–1,200 cal year

BP (Fig. 9e) followed by a gradual decline until the present day is also consistent with written sources that describe a surge in silver production that reached a peak during the Nanzhao and Dali periods (1,212–697 cal year BP). The CE 1917 Dali gazetteer mentions defunct silver mines in the Erhai area, but there is no obvious mention of silver production in Ming or Qing times, which is consistent with the sediment record.

The fourth impact phase (500–200 cal year BP) is defined by the largest peak in open/disturbed land pollen taxa, reaching nearly 30% of total arboreal pollen at ~400 cal year BP before declining to the present day (Fig. 9c). The sediment response curves describe peak influxes of topsoil, gully-derived material (Fig. 9f) and basalt sources (Fig. 9d), a renewed influx of plagioclase (Fig. 9d), and a rise in high river discharge maxima (Fig. 9g). The level of sediment organic carbon declines to <2% at 500–300 cal year BP (Shen et al. 2006), also suggesting the peak flux of minerogenic material. While, intuitively, close links can be made between these processes, it is important to note that these peaks and trends are asynchronous. The order of the peaks in sediment proxies, spanning about 200 years, is as follows: open/landscape taxa; topsoil; magnetite-rich gully sediment; basalt sediment; and the high flood maxima. A key task is therefore to provide explanations for lagged responses to the climate and known human activities at this time.

The detailed documentary descriptions given by Elvin et al. (2002) highlight intensifying pressures on water supplies, flood defences and available farmland during the Ming period, and it seems that these were often intimately linked. There are many recorded water shortages, some linked to drought or unlawful actions over shared water resources, as well as flood events that destroyed land. The early Ming period actually witnessed a centennial-scale minimum in monsoon intensity (Fig. 9a: ~550–450 cal year BP), which was also characterised by extreme variability (Fig. 9b), though with apparently little response in the river discharge record. It is therefore plausible that this was a period when population expansion coincided with highly variable climate. There are certainly many references to farmers or groups of people moving into marginal (normally upland) agricultural land, indicative of a growing population, and consistent with the pollen record (Elvin et al. 2002).

Later, from  $\sim 480$  cal year BP onwards, the river discharge curve begins to exhibit increased variability, with a greater number of high flood maxima. We know that an environmental crisis was developing at this time (Elvin et al. 2002). For example, the Miju river was already dyked by about CE 1425, and by CE 1550 there was the need for regular maintenance. An account by Xu Xiake (Elvin and Crook 2003) shows that there were no noticeable hydrological difficulties around CE 1650 BP and, given the time of year he travelled (early spring), annual dredging above the Putuo gorge had not yet started. Since the sediment pollen record suggests that this time was approaching the maximum extent of agricultural land, with peak topsoil erosion, we might surmise that the channel infilling on the Miju recorded after about CE 1700 was driven by accelerated erosion. The continued rise in gully and basalt sediments reaching peaks, slightly later than the peak extent of agriculture, at  $\sim 400$ – $300$  cal year BP and  $\sim 250$  cal year BP respectively means that the number, length or depth of the gullies were also increasing. Between CE 1713 and CE 1817 there were 13 documented river breaches during the late-summer/autumn monsoonal floods, and given the sediment dating constraints this timing is consistent with the sediment record of high flood maxima trend (Fig. 9g). Thus, it appears that major gully growth, lagging behind the timings of agricultural expansion by a century or so, is a key factor in explaining the serious flooding on the Miju river.

This final phase is, however, unique in the mid-late Holocene for the strengthening, and importantly, highly variable, monsoon regime (Fig. 9a and b). Even in an undisturbed catchment, such a climate shift might have caused a change in the flooding regime. But under disturbed conditions, the impact was severe, for example: “... after [CE] 1757 and 1758 the hills in front of and behind Tower Base [above Baihan] were gradually opened up for farming. These hills had neither vegetation nor trees to give them protective cover. As soon as there was a heavy rain, the sediments and stones came down in a transverse fashion and obliterated the dry cross-dyke with their pressure, striking and choking the body of the river ....” (quoted in Elvin et al. 2002). Such was the impact of these practises in the Baihan valley, in the Eryuan basin, that in CE 1762 a 1 km cross-dyke was built to trap sediments before they reached the Miju river. Other evidence also points to the

destabilization of slopes and enhanced sediment loads. For example, our observations of channel sequences close to the northeastern shore show  $>1.5$  m aggradation of fine red sediment, coarsening upwards to gravel-sized clasts, above two ‘modern’  $^{14}\text{C}$  dated charcoal samples (Beta-155410/155411:  $<300$  cal year BP), and progradation of the Miju delta reached a maximum of  $\sim 0.2$  km/year during the mid-19th century (Elvin et al. 2002).

Whether or not these responses were linked to the change in monsoon regime, or were essentially the product of poor land management practises is difficult to ascertain. Comparison of the monsoon and flood records through the phase suggests that the trend of high flood maxima tracks the trends in both increasing monsoon intensity and variability, while the low flood maxima stay low throughout. On the millennial-scale (Fig. 6h), the magnitude of the high flood proxies is well below the level recorded in the mid-Holocene when the monsoon was weakening. Thus the argument could be made that the sediment record of river discharge, while tracking the change in monsoon regime, was actually suppressed in terms of magnitude. Testing this hypothesis would require quantitative proxy calibration, and an improved sediment chronology, but if true, would reaffirm the significant hydrological impact of paddy field farming on flooding.

The sediment dating uncertainties means that it is difficult to make valid comparisons between the sediment and historical records within the last 200 years. We may speculate that declines in the sediment record of gully erosion since  $\sim 400$  cal year BP (Fig. 9f) may be linked to reduced exploitation of steep slopes generally and recent attempts at land conservation measures. However, the continuing high levels of soil erosion (Fig. 9f) are consistent with the relatively recent establishment of small village settlements on some summits and ridge tops that continue to generate runoff and sediment from cultivated fields. The very recent upturn in the magnetite proxy for gully erosion (Fig. 9f) also opens up the possibility of renewed gully activity, as yet unexplained.

## Discussion

The reconstructions reveal the range and complexity of climate–human–environment interactions over at

least 7,500 years. This final section returns to the questions posed at the outset to consider how learning from environmental archives (cf. Dearing et al. 2006b) gives insight into how the lake-catchment behaves as a system, thus helping to define the critical system properties that underlie sustainability.

How sensitive are the studied environmental system processes to climate and human drivers of change?

In terms of sensitivity to climate, studying the direct effect of temperature at Erhai is hampered by the lack of a local temperature time-series for the Holocene. However, the conditions and processes that have showed direct sensitivity to early changes in temperature are runoff, flooding and forest composition before the thermal maximum. During this period it seems that changes in both the annual mean and seasonality of temperature controlled the competitiveness of certain functional ecological groups, such as broadleaved evergreen forest, and may have affected the level of snow accumulation and snow-melt. Assessing the sensitivity of processes to the intensity of the summer monsoon is more certain. Certainly, the millennial-scale weakening of the monsoon led to the decline of certain sensitive species, such as *Tsuga*, and seems to have driven the trend in low flood minima, even through periods of human activity. The high frequency (inter-centennial scales) flood record has also been shown to be sensitive to phases of high monsoon variability.

In terms of human impact, the terrestrial ecosystems have been modified by deforestation and pastoralism (and by implication burning), cultivation, irrigation and urbanisation embracing all sectors and altitudinal zones of the catchment. Later phases of cultivation or overgrazing on high and steep slopes clearly led to accelerated surface erosion processes followed by gully, and intensified metal workings drove enhanced levels of metal contaminated particulates through the fluvial system. However, many process-responses in the mid-late Holocene were sensitive to a *combination* of climate and human activities, particularly where land use and hydraulic engineering were the predominant human activities mediating flood, erosion and sediment transport records. For some process-responses the actual

system behaviour was strongly linked to the type of mediating land use. For example, the flood response was highly sensitive to initial deforestation, triggering high flood maxima. Whereas the impact of irrigation practices on flooding, seemingly by widening the variance between low and high discharge events, compounded the effects of a weakening monsoon. Although these processes are directly affected by climate, the record strongly points to human activities as the first order control. One exception may be the early phases of increased gully erosion and the transport of heavy metals for which tectonic or climate control alone cannot be ruled out.

The biotic and hydrogeomorphic response proxies in this study include vegetation, sediment sources, soil erosion, heavy metal transport and flooding. But which has been most affected by human–climate forcings? Attempts to classify proxies according to a quantifiable amount of transformation over the Holocene are compromised by different units of measurement, calibration, linearity and changes in sedimentation rate that makes valid comparison difficult. However we might argue that surface soil erosion (as indicated by frequency-dependent susceptibility) from ~1,600 cal year BP should be ranked highest as it is unique in terms of its *emergence* during the Holocene. It is a proxy that captures many different soil types and, though quantitatively difficult to calibrate in terms of erosion rates, describes a late-Holocene trajectory that is highly consistent with the documented history of land use. Such a conclusion does not necessarily imply that it is the most important change by other definitions, such as hazard risk or water quality, but it does mark a fundamental threshold transgression and seemingly a shift to irreversible system conditions.

Can we observe long-term trajectories of socio-environmental interactions, or periods of social collapse and recovery?

The term ‘trajectory of vulnerability’ was coined by Messerli et al. (2000) to describe a sequence of human–environment interactions leading to system behaviour that is ‘human-dominated’. It provides a useful template for classifying and describing the evolution of socio-environmental interactions.

Messerli et al. (2000) argue that human-dominated systems are those where societies and economies are increasingly vulnerable to extreme events and natural variability. At Erhai, we can make a number of relevant observations. There is evidence in the lake and terrestrial sediment records for a 'human-affected environment' as early as  $\sim 9,000$  cal year BP, but when was the switch to a human-dominated system? In ecological terms, we might point to  $\sim 4,800$  cal year BP when major deforestation/grazing led to not only the demise of certain individual forest species but also ecological functional units. But in hydrology terms, the switch may be linked to the later introduction of paddy field irrigated farming, certainly by 2,000 cal year BP, and in geomorphic terms we might identify the exploitation of mountain slopes  $\sim 1,600$  cal year BP that led to surface erosion and gully. In each case, human impacts may have caused irreversible changes to the functioning of key processes within the lake-catchment system, though analysis of each suggests quite different combinations of social and climate drivers.

The earliest of these cases probably represents the dispersion of the population away from the established sedentary agricultural units on alluvial fans to the more inhospitable margins of the lake and the valleys. This perhaps signifies the end of the 'nature-dominated' phase (Messerli et al. 2000) where society could cause significant modification of the landscape but was still vulnerable to the main risks of drought and flood (though the evidence for climate determinism is weak). In contrast, the introduction of irrigation is associated with a trend of weakening monsoon intensity, increasing numbers of centennial-scale dry phases, and population growth. It represents an agrarian society in transition, using technological innovation to raise carrying capacities without increasing greatly the vulnerability to drought or flood. The third period is linked to natural population growth, inward migration and metal extraction brought about by the rise of Nanzhao/Dali as a major centre.

Despite the *apparent* suppression of high flood maxima over the past 500 years, in the proxy record, flooding has been one of the most documented hazards in the Miju valley. It is a contradiction that serves to underline not just the gradual failure of the hydrological/hydraulic systems to operate as efficient adaptive mechanisms but the social perceptions and

relative definitions of hazard, risk and vulnerability. The Ming environmental crisis was caused by a growing sensitivity of the environment to extreme events caused by, what has been termed (Homer-Dixon 2006), a 'convergence of stresses': the culmination of centennial-scale trajectories in reduced land cover, increased soil erosion, and increased gully erosion driven by the exploitation of agriculturally marginal lands (illegal deforestation, unsustainable terraced agriculture and over-grazing) without the appropriate renewal or strengthening of adaptive capacity. Higher monsoonal intensities and variance at this time may have triggered the crisis, but the role of climate in driving environmental change was subordinate to social change.

At this point, we can usefully make the connection between the observed trajectories and resilience theory (Gunderson and Holling 2002), and ask: where does the modern Erhai socio-ecological system lie on an adaptive cycle? Adaptive cycles track the evolutionary nature of systems as they pass through periods of growth (r), conservation (K), release ( $\Omega$ ) and reorganisation ( $\alpha$ ). For example, as soil and substrates weather they accumulate nutrients and aggregated particles (K) that may become released through erosive processes ( $\Omega$ ), followed by reorganisation ( $\alpha$ ) to stable but shallower profiles, and growth through renewed weathering (r). At Erhai (Dearing 2008), the slow processes of weathering and soil accumulation, in association with vegetation cover held fairly constant by a benign early-mid Holocene climate, were interrupted by fast processes of anthropogenic modification of vegetation. For many centuries, this concatenation of 'slow-long' and 'fast-short' processes led to a resilient land use-soil system (cf. Gunderson and Holling 2002). But increasing perturbations led to system failure, and we can observe that the late Ming environmental crisis represents the end of the last release phase ( $\Omega$ ). Thus, the modern landscape may be approaching a conservation phase (K) characterised by minimum resilience.

What are the implications for modern system functioning and future sustainability?

In systems terms, the modern Erhai agrarian system, like many world landscapes, is a 'dissipative system'

in disequilibrium. The sediment records show that despite some recovery from the Ming/Qing crisis, the environmental processes recorded at the modern time, for example surface soil erosion (Fig. 9f), lie on trajectories far removed from base-line levels in the early-mid Holocene before major disturbance. Dissipative systems are often considered resilient to moderate perturbations but disproportionately sensitive to extreme perturbations. Continued levels of resilience and stability are theoretically dependent on continued throughflows of energy, which at Erhai are mainly water, labour and fertilizers. A systems viewpoint would argue that adaptation to new social and climate forces requires that the throughflows should be continually maintained, for example, by constructing new or reconstructing hillslope terraces, irrigation channels and dykes. If a decline in these throughflows is unavoidable or desirable, there needs to be a matched reduction in the dependency on the human-modified landscape.

However the historical perspective gives greater insight into the modern system. First, although the disequilibrium state has existed for at least 5,000 years, there is no strong evidence of centennial-scale social collapse and migration caused directly by climate. Far more evident is the environmental degradation and partial social collapse seen over the last 1,000 years driven by failure to maintain carrying and adaptive capacities in the face of social drivers of change. Second, it shows that the modern socio-environment sits on a continuing system trajectory which functions through a set of interacting processes. Importantly, these processes, both social and ecological, possess different directions, time-spans, rates of change and levels of historical contingency. For example, at the present time, the trajectory of topsoil erosion seems to be declining, while that of gullying seems to be increasing (Fig. 9f). Furthermore, 1,500 years of gullying has created a massive storage of sediment on lower slopes, alluvial fans, channels and in river deltas that current plans for flood defences and lake water quality have to take into account. Sediment movement through slope-channel systems is an important 'slow-long' process in the modern landscape. In contrast, it is difficult to discern a centennial-scale trajectory for high maxima floods (Fig. 9g), as they probably respond to drivers operating over a range of timescales from hours to centuries: the most obvious

'fast-short' processes. And third, if we apply the 'adaptive cycle' to the land use-gully erosion system, we would deduce that maximum resilience was reached  $\sim 100$  years ago during the last phases of reorganization and growth. The important corollary is that the apparent stability of the modern conservation phase warrants caution as it is defined by minimum resilience.

In terms of the continued sustainability of local agriculture (subsistence and market) the largest environmental threat over the past 1,500 years has come from high magnitude-low frequency flooding of lower dry farmed terraces and the irrigated valley plain, and this threat continues today. Such flooding may be driven or exacerbated in the future by:

- (a) continued use of high altitude and steep slopes for grazing and cultivation that generate high runoff from unprotected slopes and maintain active gully systems, particularly in the northern basins;
- (b) reduction or poor maintenance of paddy field systems, engineered flood defences, river channels and terraces;
- (c) increased intensities of the summer monsoon.

With respect to the last point,  $\geq 66\%$  of climate simulations using AR4 AOGCM (A1B scenario) project increases in total precipitation for this region by 2080–2099, and an increase in precipitation 'extremes' is defined as 'likely' (Christensen et al. 2007, p. 859). More generally, a recent review (Dearing et al. 2006c) of centennial-scale socio-environmental interactions emphasizes the potential vulnerability of many modern agricultural systems. Many are approaching, or have reached, a state of hyper-coherence or 'brittleness' where maintaining continued resilience to external perturbations becomes increasingly difficult and costly. At Erhai, such a state was last reached more than 500 years ago but may, at least for the land use-soil system, be approaching a similar state today. While the study shows the historical consequences of failing to maintain resilience, it also provides the foundation for formulating appropriate land management strategies to avoid history repeating itself.

**Acknowledgements** This study was funded and supported by the Leverhulme Trust (Grant No. F00025/E), the National Nature Science Foundation of China (Grant No. 40331003), the

Chinese Academy of Sciences (Grant No. KZCX1-10-01), and the Royal Society (London). It represents a contribution to the IGBP-PAGES PHAROS Programme 'Past Human–Climate–Ecosystem Interactions' that seeks to inform about the sustainable management of environmental systems from studies of past ecosystems. We thank Jiang Xuezhong, Xia Weilan, Wu Yanhong, Zhang Enlou and Zhang Gaoping for help during fieldwork; Carolyn Dykoski and Sun Donghuai for discussions about Asian monsoon records; Eldon Worrall for help in dating ceramics; Masayuki Hyodo for making available susceptibility data from core ER3; and Frank Oldfield for insightful comments on a previous version of the paper. As ever, many thanks go to Sandra Mather for her excellent artwork.

## References

- Allen CR, Gillespie AR, Han Y, Sieh KE, Zhang B, Zhu C (1984) Red River and associated faults, Yunnan Province, China: quaternary geology, slip rates, and seismic hazard. *Geol Soc Am Bull* 95:686–700
- Anderson NJ, Bugmann H, Dearing JA, Gaillard-Lemdhall M-J (2006) Linking palaeoenvironmental data and models to understand the past and to predict the future. *Trends Ecol Evol* 21:696–704
- Boyle JF (2001) Inorganic geochemical methods in palaeolimnology. In: Last WM, Smol JP (eds) *Tracking environmental change using lake sediments: physical and chemical techniques*. Kluwer Academic, Dordrecht, pp 83–141
- Bradshaw EG, Nielsen AB, Anderson NJ (2006) Using diatoms to assess the impacts of prehistoric, pre-industrial and modern land-use on Danish lakes. *Reg Environ Change* 6:17–24
- Brenner M, Dorsey K, Xueliang S, Zuguan W, Ruihua W, Binford M, Whitmore TJ, Moore AM (1991) Paleolimnology of Qilu Hu, Yunnan Province, China. *Hydrobiologia* 214:333–340
- Bureau of Geology, Mineral Resources of Yunnan Province (1990) *Regional geology of Yunnan Province*. Geological Publishing House, Beijing, 728 pp
- Chen X, Yu G, Liu J (2002) Paleoclimate simulation of mid Holocene for East Asia, and discussion of the temperature change. *Sci China Ser D* 32:335–345
- Chen J, Wan G, Zhang DD, Chen Z, Xu J, Xiao T, Huang R (2005) The 'Little Ice Age' recorded by sediment chemistry in Lake Erhai, southwest China. *Holocene* 15: 925–931
- Christensen JH, Hewitson B, Busuioac A, Chen A, Gao X, Held I, Jones R, Kolli RK, Kwon W-T, Laprise R, Magaña Rueda V, Mearns L, Menéndez CG, Räisänen J, Rinke A, Sarr A, Whetton P (2007) Regional climate projections. In: Solomon S, Qin D, Manning M, Chen Z, Marquis M, Averyt KB, Tignor M, Miller HL (eds) *Climate change 2007: the physical science basis*. Contribution of working group I to the fourth assessment report of the intergovernmental panel on climate change. Cambridge University Press, Cambridge
- Dearing JA (1997) Sedimentary indicators of lake-level changes in the humid temperate zone: a critical review. *J Paleolimnol* 18:1–14
- Dearing JA (1999) Holocene environmental change from magnetic proxies in lake sediments. In: Maher BA, Thompson R (eds) *Quaternary climates, environments and magnetism*. Cambridge University Press, Cambridge, pp 231–278
- Dearing JA (2006) Climate–human–environment interactions: resolving our past. *Clim Past* 2:187–203
- Dearing JA (2008) Landscape change and resilience theory: a palaeoenvironmental assessment from Yunnan, SW China. *Holocene* 18:117–127
- Dearing JA, Zolitschka B (1999) System dynamics and environmental change: an exploratory study of Holocene lake sediments at Holzmaar, Germany. *Holocene* 9:531–540
- Dearing JA, Dann RJL, Hay K, Lees JA, Loveland PJ, Maher BA, O' Grady K (1996) Frequency-dependent susceptibility measurements of environmental samples. *Geophys J Int* 124:228–240
- Dearing JA, Hannam JA, Huddleston AS, Wellington EMH (2001) Magnetic, geochemical and DNA properties of highly magnetic soils in England. *Geophys J Int* 144: 183–196
- Dearing JA, Battarbee RW, Dikau R, Larocque I, Oldfield F (2006a) Human–environment interactions: learning from the past. *Reg Environ Change* 6:1–17
- Dearing JA, Battarbee RW, Dikau R, Larocque I, Oldfield F (2006b) Human–environment interactions: towards synthesis and simulation. *Reg Environ Change* 6:115–123
- Dearing JA, Graumlich LJ, Grove R, Grübler A, Haberl H, Hole F, Pfister C, van der Leeuw SE (2006c) Integrating socio-environment interactions over centennial time-scales: needs and issues. In: Costanza R, Graumlich L, Steffen W (eds) *Integrated history and future of people on earth*. Dahlem workshop report 96. The MIT Press, Cambridge, pp 243–274
- Deevey ES Jr (1984) Stress, strain and stability of lacustrine ecosystems. In: Haworth EY, Lund JWG (eds) *Lake sediments and environmental history*. Leicester University Press, pp 203–229
- Dykoski CA, Edwards RL, Cheng H, Daoxian Y, Cai Y, Zhang M, Lin Y, Qing J, An Z, Revenaugh J (2005) A high resolution, absolute-dated Holocene and deglacial Asian monsoon record from Dongge Cave, China. *Earth Planet Sci Lett* 233:71–86
- Elvin MJD, Crook DS (2003) An argument from silence? The implications of Xu Xiake's description of the Miju river in 1639. In: Yunnan University History Department (eds) *Anthology of essays in commemoration of Professor Li Ting's ninetieth birthday*. Yunnan University Press, Kunming, 3 pp
- Elvin MJD, Crook DS, Jones RT, Dearing JA (2002) The impact of clearance and irrigation on the environment in the lake Erhai catchment from the ninth to the nineteenth century. *East Asian Stud* 23:1–60
- Fang JQ (1991) Lake evolution during the past 30,000 years in China, and its implications for environmental change. *Quaternary Res* 36:37–60
- Foster DR, Swanson F, Aber J, Burke I, Brokaw N, Tilman D, Knapp A (2003) The importance of land-use legacies to ecology and conservation. *Bioscience* 53:77–88
- Gunderson LH, Holling CS (eds) (2002) *Panarchy: understanding transformations in human and natural systems*. Island Press, Washington, 507 pp

- Guodong Z, Takano B, Kuno A, Matsuo M (2001) Iron speciation in modern sediment from Erhai Lake, southwestern China. Redox conditions in an ancient environment. *Appl Geochem* 16:1201–1213
- Higham C (2005) East Asian agriculture and its impact. In: Scarre C (ed) *The human past*. Thames and Hudson, London, pp 234–263
- Hodell DA, Brenner M, Kanfoush SL, Curtis JH, Stoner JS, Song XL, Wu Y, Whitmore TJ (1999) Paleoclimate of southwestern China for the past 50,000 yr inferred from lake sediment records. *Quaternary Res* 52:369–380
- Homer-Dixon T (2006) *The upside of down: catastrophe, creativity and renewal of civilisation*. Island Press, Washington, 448 pp
- Hu WY, Hu HY, Pan HX (1989) Chemical characteristics of water in Erhai Lake. In: Shen LX (ed) *Collected scientific works on Erhai Lake in Yunnan*. Yunnan National Press, Yunnan, pp 118–128 (in Chinese)
- Hyodo M, Yoshihara A, Kashiwaya K, Okimura T, Masuzawa T, Nomura R, Tanaka S, Xing TB, Qing LS, Jian LS (1999) A late Holocene geomagnetic secular variation record from Erhai Lake, southwest China. *Geophys J Int* 136:784–790
- Institute of Archaeology, Yunnan Province (1990) Excavations of ancient tombs on Aofengshan hill, Jianchuan County, Yunnan. *Acta Archaeologica Sinica* 2:239–265 (in Chinese)
- Institute of Botany, CAS (1960) *Plant pollen morphology of China*. Science Press, Beijing (in Chinese)
- Institute of Botany, CAS (1976) *Sporae pteridophytorum sinicarum*. Science Press, Beijing (in Chinese)
- Institute of Botany, South China Institute of Botany, CAS (1982) *Angiosperum pollen flora of tropic and subtropic China*. Science Press, Beijing (in Chinese)
- Jarvis DI (1993) Pollen evidence of changing Holocene monsoon climate in Sichuan Province, China. *Quaternary Res* 39:325–337
- Johnson KR, Ingram BL (2004) Spatial and temporal variability in the stable isotope systematics of modern precipitation in China: implications for paleoclimate reconstructions. *Earth Planet Sci Lett* 220:365–377
- Kharakwal JS, Yano A, Yasuda Y, Shinde VS, Osada T (2004) Cord impressed ware and rice cultivation in South Asia, China and Japan: possibilities of inter-links. *Quaternary Int* 123–125:105–115
- Lin X, Walker D (1986) The plant geography of Yunnan Province, southwest China. *J Biogeogr* 13:376–397
- Lin X, Qiao Y, Walker D (1986) Late Pleistocene and Holocene vegetation history at Xi Hu, Er Yuan, Yunnan Province, southwest China. *J Biogeogr* 13:419–440
- Liu J, Yu G, Chen X (2002) Paleoclimate simulation of 21Ka for the Tibetan Plateau and Eastern Asia. *Clim Dyn* 19:575–583
- Long R, Li B, Brenner M, Song XL (1991) A study of late Pleistocene to Holocene vegetation in the Jilu Lake area of central Yunnan. *Yunnan Geol* 10:105–118 (in Chinese)
- Messerli B, Grosjean M, Hofer T, Núñez L, Pfister C (2000) From nature-dominated to human-dominated environmental change. *Quaternary Sci Rev* 19:459–479
- Moberg A, Sonechkin DM, Holmgren K, Datsenko NM, Karlén W (2005) Highly variable Northern Hemisphere temperatures reconstructed from low- and high-resolution proxy data. *Nature* 453:613–617
- Oldfield F, Dearing JA (2003) The role of human activities in past environmental change. In: Alverson K, Bradley R, Pedersen T (eds) *Paleoclimate, global change and the future*. IGBP Synthesis Book Series, Springer Verlag, pp 143–162
- Pelejero C, Grimalt JO, Heilig S, Kienast M, Wang L (1999) High resolution UK<sup>37</sup>-temperature reconstructions in the South China Sea over the past 220 kyr. *Paleoceanography* 14:224–231
- Scheffer M, Carpenter SR (2003) Catastrophic regime shifts in ecosystems: linking theory to observation. *Trends Ecol Evol* 18:648–656
- Shen J, Yang L, Yang X, Matsumoto R, Tong G, Zhu Y, Zhang Z, Wang S (2005) Lake sediment records on climate change and human activities since the Holocene in Erhai catchment, Yunnan Province, China. *Sci China Ser D Earth Sci* 48:353–363
- Shen J, Jones RT, Yang X, Dearing JA, Wang S (2006) The Holocene vegetation history of Erhai Lake, Yunnan Province southwestern China: the role of climate and human forcings. *Holocene* 16:265–276
- Socquet A, Pubellier M (2005) Cenozoic deformation in western Yunnan (China-Myanmar border). *J Asian Sci* 24:495–515
- Sun X, Wu Y, Qiao Y, Walker D (1986) Late Pleistocene and Holocene vegetation history at Kunming, Yunnan Province, southwest China. *J Biogeogr* 13:441–476
- Sun S, Zhang C, Eisma D, Thomasse E, Song XL (1999) Recent sedimentation and suspended matter in Erhai lake, Yunnan Province, China. *Chin J Oceanol Limnol* 17:1–8 (in Chinese with English abstract)
- Tan M, Cai B (2005) Preliminary calibration of stalagmite oxygen isotopes from eastern monsoon China with Northern Hemisphere temperatures. *PAGES Newsl* 13:16–17
- Walker D (1986) Late Pleistocene-early Holocene vegetational and climatic changes in Yunnan Province, southwest China. *J Biogeogr* 13:477–486
- Wang E (ed) (1998) *Late Cenozoic Xianshuihe-Xiaojiang, Red River, and Dali fault systems of southwestern Sichuan and central Yunnan, China*. The Geological Society of America, Special Paper 327. Boulder, Colorado, 106 pp
- Wang J, Lu H, Shen C (1990) Factor interpretation method and quantitative analysis of climatic changes over the past 12,000 years in China. In: Lu C et al (eds) *Global changes and environmental evolution in China*. Science Press, Beijing, pp 63–68 (in Chinese with English abstract, cited by He Y, Theakstone WH, Zhang Z, Zhang D, Yao T, Chen T, Shen Y, Pang H (2004) Asynchronous Holocene climatic change across China. *Quaternary Res* 61:52–63)
- Wang F, Qian N, Zhang Y, Yang H (1995) *Plant pollen morphology of China*, 2nd edn. Science Press, Beijing (in Chinese)
- Wang X, Yu S, Huang GH (2004) Land allocation based on integrated GIS optimization modeling at a watershed level. *Landsc Urban Plan* 66:261–274
- Wang Y, Cheng H, Edwards RL, He Y, Kong X, An Z, Wu J, Kelly MJ, Dykoski CA, Li X (2005) The Holocene Asian Monsoon: links to solar changes and North Atlantic climate. *Science* 308:854–857

- Whitmore TJ, Brenner M, Engstrom DR, Song XL (1994) Accelerated soil erosion in watersheds of Yunnan Province, China. *J Soil Water Conserv* 49:67–72
- Whitmore TJ, Brenner M, Jiang Z, Curtis JH, Moore AM, Engstrom DR, Wu Y (1997) Water quality and sediment geochemistry in lakes of Yunnan Province, southern China. *Environ Geol* 32:45–55
- Wu Z, Zhu Y, Jiang H (1987) *Vegetation of Yunnan Province*. Science Press, Beijing (in Chinese)
- Xu S, Zheng G (2003) Variations in radiocarbon ages of various organic fractions in core sediments from Erhai Lake, SW China. *Geochem J* 37:135–144
- Yang B (2004a) Military campaigns against Yunnan: a global analysis working paper series No. 30. Asia Research Institute, National University of Singapore
- Yang B (2004b) Horses, silver and cowries: Yunnan in global perspective. *J World Hist* 15:281–322
- Yu L, Oldfield F, Wu Y, Zhang S, Xiao J (1990) Paleoenvironmental implications of magnetic measurements on sediment core from Kunming Basin, Southwest China. *J Paleolimnol* 3:95–111
- Yu G, Harrison SP, Xue B (2001) Lake status records from China: data base documentation. Technical reports—Max-Planck-Institute für Biogeochemie 4, 243 pp
- Zhang Z (1990) *Archaeology of the peoples of southwest China*. Yunnan Museum Research Series. Yunnan People's Publishing House, Kunming (in Chinese)
- Zhu HH (ed) (1989) *Sediments and environments of fault lake in Yunnan Province*. Science Press, Beijing, pp 185–200 (in Chinese)